Virology 384 (2009) 38–50

Contents lists available at ScienceDirect

Virology

journal homepage: www.elsevier.com/locate/yviro

The P0 gene of *Sugarcane yellow leaf virus* encodes an RNA silencing suppressor with unique activities

Tichaona Mangwende [a,1,2], Ming-Li Wang [a,1], Wayne Borth [b], John Hu [b], Paul H. Moore [c], T. Erik Mirkov [d,*], Henrik H. Albert [c,*,3]

[a] *Hawaii Agriculture Research Center, Aiea, HI 96701, USA*
[b] *University of Hawaii, Department of Plant and Environmental Protection Sciences, Honolulu, HI 96822, USA*
[c] *USDA ARS Pacific Basin Agriculture Research Center, Aiea, HI 96701, USA*
[d] *Texas A&M University AgriLife Research Center, Department of Plant Pathology and Microbiology, Weslaco, TX 78596, USA*

ARTICLE INFO

Article history:
Received 21 July 2008
Returned to author for revision
25 September 2008
Accepted 13 October 2008
Available online 30 November 2008

Keywords:
P0
PTGS
RNA silencing
Suppressor
Cell death phenotype
Poleroviruses
Systemic PTGS

ABSTRACT

The *Sugarcane yellow leaf virus* (SCYLV) P0, a member of the highly heterologous proteins of poleroviruses, is a suppressor of posttranscriptional gene silencing (PTGS) and has additional activities not seen in other P0 proteins. The P0 protein in previously tested poleroviruses (*Beet western yellows virus* and *Cucurbit aphid-borne yellows virus*), suppresses local, but not systemic, PTGS induced by both sense GFP and inverted repeat GF using its F-box-like domain to mediate destabilization of the Argonaute1 protein. We now report that the SCYLV P0 protein not only suppressed local PTGS induced by sense GFP and inverted repeat GF in *Nicotiana benthamiana*, but also triggered a dosage dependent cell death phenotype in infiltrated leaves and suppressed systemic sense GFP-PTGS. Deletion of the first 15 N-terminal amino acid residues of SCYLV P0 abolished suppression of both local and systemic PTGS and the induction of cell death. In contrast, only systemic PTGS and cell death were lost when the 15 C-terminal amino acid residues were deleted. We conclude that the 15 C-terminal amino acid residue region of SCYLV P0 is necessary for suppressing systemic PTGS and inducing cell death, but is not required for suppression of local PTGS.

Introduction

Sugarcane yellow leaf virus (SCYLV), the causal agent of sugarcane yellow leaf disease (Borth et al., 1994; Comstock et al., 1998; Rott et al., 2008; Schenk et al., 1997; Vega et al., 1997), is a member of the *Luteoviridae* family, and has apparently arisen through recombination between a *Polerovirus*, a *Luteovirus*, and an *Enamovirus* (Moonan et al., 2000). The 5′-part of the SCYLV genome is of *Polerovirus* origin (Smith et al., 2000); the first open reading frame (ORF) in poleroviruses is termed P0. The deduced amino acid sequence of P0 proteins is highly conserved among different geographic isolates of SCYLV (Abu Ahmad et al., 2006). However the amino acid sequence identity between polerovirus P0s is very low. The best match of SCYLV P0 ($P0^{SC}$) to any other *Polerovirus* P0 is to *Potato leaf roll virus* (PLRV) P0 ($P0^{PL}$) which has 21% sequence identity. Despite the wide sequence differences, the P0 proteins of three tested poleroviruses (*Beet western yellows virus* (BWYV), PLRV, and *Cucurbit aphid-borne yellows virus* (CABYV)) are all suppressors of local posttranscriptional gene silencing (PTGS) (Pfeffer et al., 2002). The CABYV P0 ($P0^{CA}$) and BWYV P0 ($P0^{BW}$) suppressor proteins contain an F-box-like domain that is required for suppressor activity (Pazhouhandeh et al., 2006); these proteins suppress PTGS by destabilizing Argonaute1 (Ago1) protein (Baumberger et al., 2007; Bortolamiol et al., 2007).

Agrobacterium-mediated co-infiltrations of sense GFP (sGFP) with $P0^{BW}$, $P0^{PL}$, or $P0^{CA}$ led to the suppression of local PTGS in GFP transgenic *N. benthamiana*. However, systemic silencing was not suppressed. The GFP in systemic leaves showed "vein proximal silencing" at 15 d post-infiltration (d.p.i.) that spread throughout the entire leaves over time (Pfeffer et al., 2002). Both $P0^{BW}$ and $P0^{CA}$ also suppressed PTGS induced by dsGF or "GFFG" in wild type *N. benthamiana* (Baumberger et al., 2007). We now report that the $P0^{SC}$ protein has unique RNA silencing activities in addition to suppressing local sGFP-PTGS and dsGF-PTGS. In contrast to $P0^{BW}$, $P0^{PL}$, and $P0^{CA}$, $P0^{SC}$ causes a dosage-dependent cell death phenotype in the infiltrated areas of *N. benthamiana* leaves as early as

* Corresponding authors. E. Mirkov is to be contacted at Texas A&M University AgriLife Research Center, 2415 East Hwy. 83. Weslaco, TX 78596, USA. H. Albert, Pioneer Hi-Bred, 700A Bay Road, Redwood City, California, CA 94063-2478, USA.
E-mail addresses: tmangwende@gmail.com (T. Mangwende), Mwang@harc-hspa.com (M.-L. Wang), borth@hawaii.edu (W. Borth), johnhu@hawaii.edu (J. Hu), paul.moore@ars.usda.gov (P.H. Moore), e-mirkov@tamu.edu (T.E. Mirkov), HENRIK.ALBERT@PIONEER.COM (H.H. Albert).
[1] These authors contributed equally to this work.
[2] Present address: University of Pretoria, Department of Biochemistry, Pretoria 0002, South Africa.
[3] Present address: Pioneer Hi-Bred, 700A Bay Road, Redwood City, California, CA 94063-2478, USA.

0042-6822/$ – see front matter © 2008 Elsevier Inc. All rights reserved.
doi:10.1016/j.virol.2008.10.034

1 d.p.i. and it suppresses systemic sGFP-PTGS. In addition, while P0^{BW} and P0^{CA} are strong suppressors of local dsGF-PTGS, P0^{SC} has limited suppressing activity which diminishes beyond 6 d.p.i. and is accompanied by a delayed cell death phenotype in the infiltrated leaves. We also show through P0^{SC} deletion analysis that the C-terminal 15 amino acid residues are required for suppression of systemic sGFP-PTGS and induction of the cell death phenotype.

Results

We examined whether P0^{SC}, from a monocot-infecting virus, was a suppressor of PTGS like the characterized P0 proteins from dicot-infecting poleroviruses (Pfeffer et al., 2002). Since various suppressor proteins act at different stages of the silencing pathway to protect target mRNA from PTGS directed degradation, the stage at which P0^{SC} acted was also investigated. We also mapped, through deletion analysis, the regions of P0^{SC} that are required for suppressor activity (Fig. 1). P0^{SC} and deletion constructs were tested in a preliminary screen using *Agrobacterium* leaf infiltration assays in *N. benthamiana* (Johansen and Carrington, 2001; Llave et al., 2000). We selected full-length P0^{SC}, Δ2, Δ2–15, Δ69–90, Δ148–256, Δ241–256 and Δ255–256 deletions for further analysis based on the results summarized in Fig. 1.

P0^{SC} suppresses local sGFP-PTGS and induces cell death

The use of sGFP to induce PTGS requires a dsRNA intermediate that is acted on by RNaseIII-like dicers to produce 21–24 nt siRNAs. The dsRNA is formed by the action of RDR6 and cofactors on various single stranded RNAs (Curaba and Chen, 2008; Luo and Chen, 2007; Wassenegger and Krczal, 2006). Wild-type (WT) *N. benthamiana* leaves infiltrated with sGFP plus empty vector (MT), the positive control for induction of PTGS, showed GFP fluorescence that had already declined by 3 d.p.i (Fig. 2A, MT). In contrast, p19, P0^{CA}, P0^{SC} and P0^{SC} deletions (Δ2, Δ2–15, Δ69–90, Δ148–256, Δ241–256 and Δ255–256) had levels of varying PTGS suppressor activity (Fig. 2A). However, p19, P0^{CA}, P0^{SC}, Δ2, Δ241–256 (and Δ212–256, Δ226–256; not shown) and Δ255–256 all had high levels of GFP fluorescence that persisted well after 6 d.p.i. unlike Δ2–15, Δ69–90 and Δ148–256. The differences in suppressor activities indicated that the various deletions caused a partial loss of activity. Intriguingly, P0^{SC}, Δ2, and Δ255–256 resulted in a cell death phenotype that was visible as early as 1 d.p.i. (Fig. 2A, see photographs taken at 3 d.p.i. under normal light). The cell death phenotype was not evident in infiltrations with P0^{CA} whose expression, like that of P0^{SC}, was driven by the CaMV35S promoter under the same conditions. To further explore the cell death phenotype, we checked for DNA laddering (a marker for programmed cell death); there was none, indicating that generalized necrosis, rather than PCD, is likely the type of cell death (results not shown).

PTGS induced by sGFP degrades target GFP mRNA thereby reducing the amount of transcripts available for translation into a fluorescent protein. Our visual observations were confirmed by northern blot analysis of GFP mRNA isolated from infiltrated leaves of *N. benthamiana* that were harvested at 3 d.p.i. (Fig. 2B, lanes 1–11). The MT infiltration that stopped fluorescing at 3 d.p.i., had the lowest levels of GFP mRNA in infiltrated leaves, followed by Δ2–15, Δ69–90 and Δ148–256 that were each slightly higher than MT controls, while constructs p19, P0^{CA}, P0^{SC}, Δ2, Δ241–256 and Δ255–256 all strongly protected GFP mRNA (compare lanes 1, 6–8 with 2–5, 9 and 10). The variation in suppressing activities between P0^{SC} and the deletion constructs was not due to instability of their expressed mRNAs which could be detected at similar levels in northern blots (Figs. 2C, lanes 4–10). In all cases the non-infiltrated control did not show any GFP or P0^{SC} mRNAs (Figs. 2B and C, lane 11).

The hallmark of PTGS is the appearance of 21–24 nt siRNAs in the silenced tissue (Hamilton and Baulcombe, 1999). These siRNAs have been analyzed using GF and P probes to determine whether P0^{SC} (and its deletions) preferentially affect the accumulation of 5′- or 3′-derived siRNAs (Boutet et al., 2003; Zhang et al., 2008). There was an equal accumulation of high levels of 21/22–24 nt GF and P siRNAs in MT (Fig. 2D, 17hEx/3hEx/16hEx, lane 1), possibly caused by the use of full length GFP to induce PTGS. It is also possible that transiently expressed GFP in the WT *N. benthamiana* background produced suitable substrates for RDR6-dependent dsRNA formation. The dsRNA produced was a good substrate for all the dicers responsible for producing the 21/22 and 24

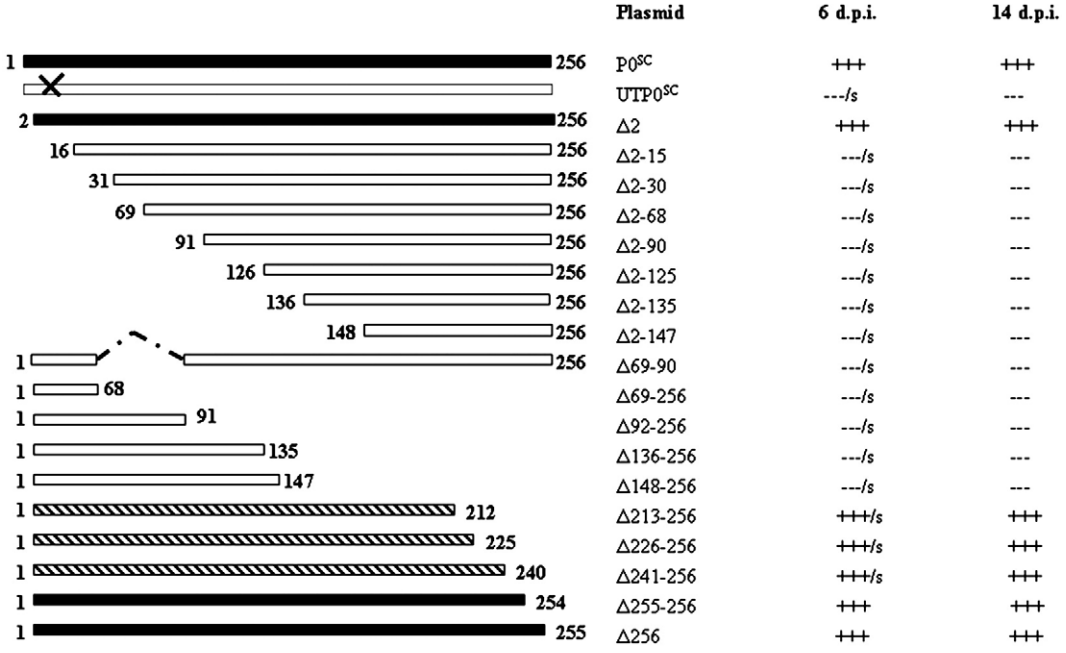

Fig. 1. Schematic representation of P0^{SC} and P0^{SC} deletion constructs that were used in the preliminary screening for suppressor activity against local sGFP-PTGS in WT and GFP transgenic *N. benthamiana* line 16c. Both local and systemic-PTGS were monitored under UV light and photographs taken at 6 and 14 d.p.i. respectively. The numbers denote the P0^{SC} amino acid residue, +++ (solid bars) are constructs with full suppressor activity, – – – (open bars) are constructs with no suppressor activity, s, systemic silencing evident at 6 d.p.i., dotted bar (UT, untranslatable mRNA, the cross is a stop codon that replaced the start codon), hatched bars, suppressor activity against local-PTGS.

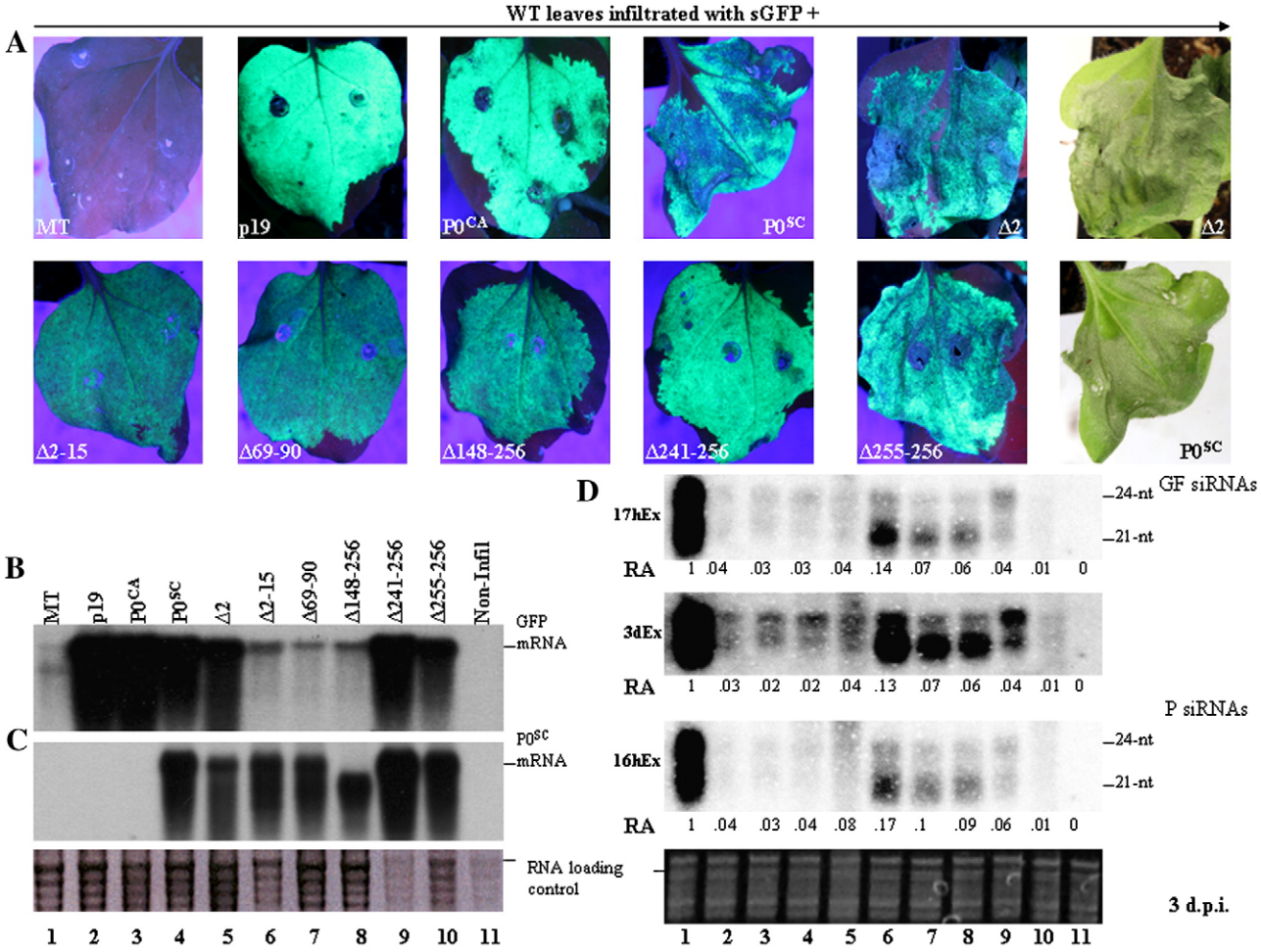

Fig. 2. (A) Agro-infiltration of WT *N. benthamiana* leaves with sGFP plus empty vector (MT), p19, P0^{CA}, P0^{SC}, Δ2, Δ2–15, Δ69–90, Δ148–256, Δ241–256 and Δ255–256 photographs were taken at 3 d.p.i. under UV illumination. The green leaf photographs taken under normal light show the cell death phenotype caused by P0^{SC}. (B) northern blot analysis of 10 μg of mRNA fractionated on 1.6% formaldehyde-agarose gel, transferred to Hybond-XL membrane and probed with radioactively labeled GFP DNA fragment. (C) Hybond-XL membrane in B was stripped and reprobed with radioactively labeled P0^{SC} DNA fragment. (D) siRNA blot probed with an *in vitro*-transcribed ^{32}P [α-dUTP] radioactive sense GF RNA, exposed for 17 h–3 d. After 3 d, the same blot was stripped and probed with an *in vitro*-transcribed radioactive sense P RNA and exposed for 16 h. The ethidium bromide stained gels show equal RNA loading. Lanes: 1, empty vector-pGD, 2, p19 positive control suppressor protein from TBSV, 3, P0^{CA} positive control suppressor protein from a polerovirus, CABYV, 4, P0^{SC} a candidate suppressor protein from SCYLV also a polerovirus, 5–10, P0^{SC} deletions Δ2, Δ2–15, Δ69–90, Δ148–256, Δ241–256 and Δ255–256) and 11, non-infiltrated sample. Note that in all Figs. where siRNAs were analysed, the RA value is the relative abundance of both size classes of the siRNAs in the infiltrated test leaf samples compared to those in the control sample (MT).

nt size classes of siRNAs. P0^{SC}, Δ2, and Δ255–256, like p19 and P0^{CA}, greatly reduced both GF and P 21/22–24 nt siRNAs (Fig. 2D, 17hEx/16hEx, lanes 2–5, 10) but did not eliminate the siRNAs completely (Fig. 2D, 3dEx, lanes 2–5, 10). Interestingly, the P0^{SC} deletions Δ2–15, Δ69–90 and Δ148–256 selectively accumulated high levels of the 21/22 nt size classes of GF and P siRNAs compared to MT (lanes 6–8, and 1). In contrast, the deletion Δ241–256 preferentially accumulated the 24 nt size class of GF and, to a lesser extent, P siRNAs (Fig. 2D, lane 9). There was a visible siRNA size shift from 21/22–24 to 22–24 nt effected by P0^{CA}, P0^{SC} and Δ241–256 in the GF siRNA blot (Fig. 2D, lanes 3, 4 and 9). In all cases, no siRNAs were found in RNAs isolated from the non-infiltrated leaves (Fig. 2D, lane 11). There was no P0^{SC} directed preference for either the 5′- or 3′-siRNAs (Fig. 2D, lane 4). Given that the GFP fluorescence, mRNA and siRNA levels for sGFP-PTGS in p19, P0^{CA} and P0^{SC} infiltrated tissues were similar, we further examined whether these suppressors similarly affected dsGF-PTGS that precluded RDR6 and cofactors in WT *N. benthamiana*.

P0^{SC} has limited suppressor activity against dsGF-PTGS

Previous studies have shown that P0^{CA} and P0^{BW} suppress PTGS induced by dsGF (GFFG) in WT *N. benthamiana* (Bortolamiol et al., 2007). We investigated the relative suppressor activities of P0^{SC} and P0^{CA} by co-infiltration experiments with sGFP plus dsGF into WT *N. benthamiana* leaves and also monitored GFP expression under UV light at 3 and 6 d.p.i. (Figs. 3A and E). The PTGS induced by dsGF effectively reduced GFP fluorescence in leaves co-infiltrated with MT even as early as 1 d.p.i. and was absent at 3 d.p.i. (Fig. 3A). Leaves infiltrated with p19 showed higher GFP fluorescence compared to either P0^{CA} or P0^{SC} (Fig. 3A). The P0^{SC} and P0^{CA} infiltrated leaves had similar GFP fluorescence at 3 d.p.i. The GFP fluorescence in P0^{SC} infiltrated leaves, like that of p19 and P0^{CA}, persisted but at very low levels beyond 6 d.p.i., suggesting only limited P0^{SC} suppressor activity against dsGF-PTGS (Fig. 3E). Intriguingly, the rapid cell death phenotype associated with P0^{SC} plus sGFP infiltrations was delayed and less necrotic (compare Figs. 3A and E, P0^{SC}, at 3 and 6 d.p.i.).

Northern blot analysis was used to determine the correlation between the observed GFP fluorescence and its mRNA. dsGF-PTGS reduced target GFP mRNA levels in MT infiltrations to barely detectable levels compared to p19, P0^{CA} and P0^{SC} (Figs. 3B, lanes 1–4 and 3F, lanes 2–5). At 6 d.p.i., P0^{SC} weakly protected GFP mRNA (Fig. 3F, lane 5) compared to p19 and P0^{CA} (Fig. 3F, lanes 3–4).

dsGF-PTGS was verified by analysis of both GF primary and P secondary siRNAs at 3 d.p.i. (Fig. 3D) and at 6 d.p.i. (Fig. 3H). In all

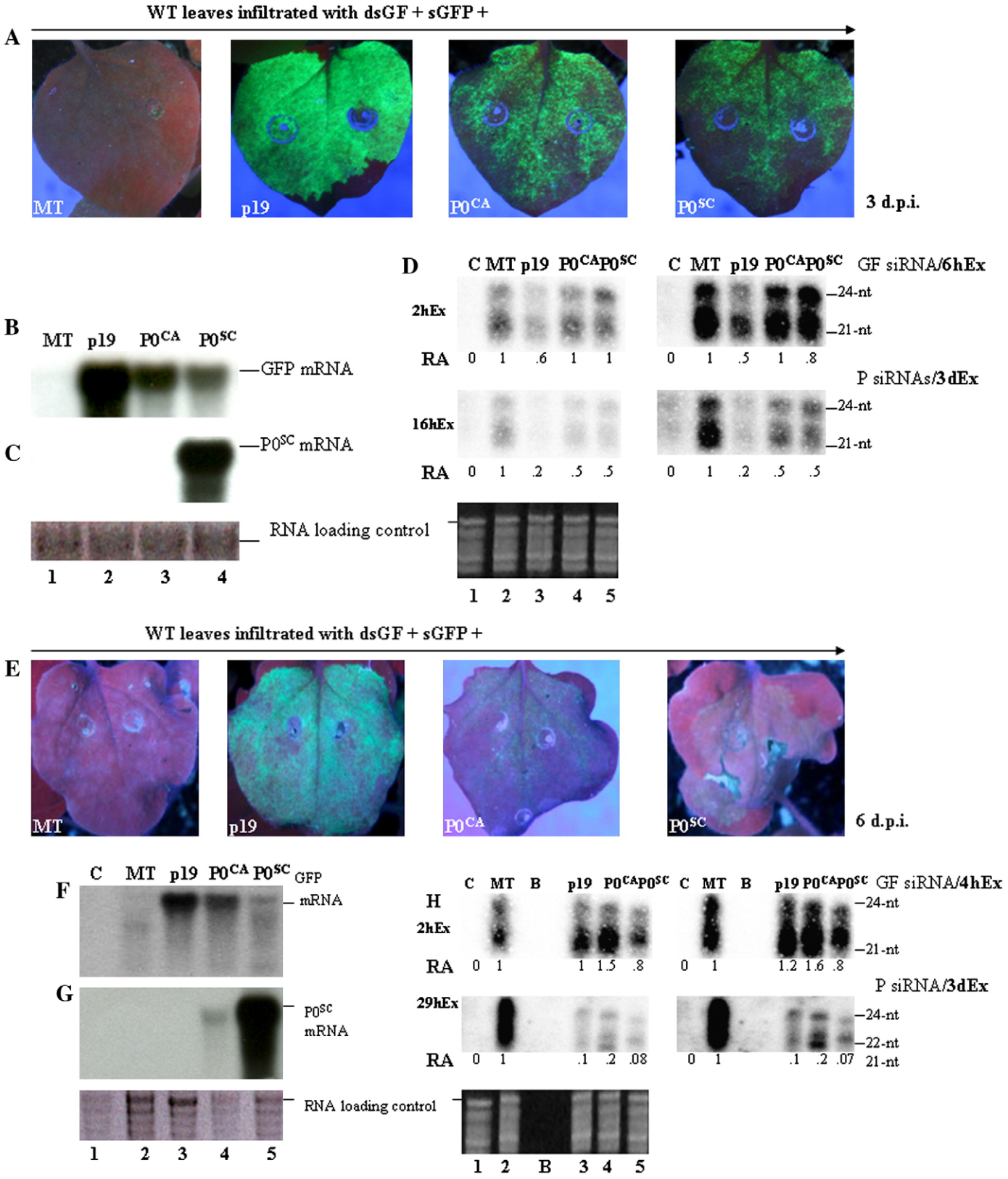

Fig. 3. (A and E) Agro-infiltration of WT *N. benthamiana* with dsGF and sGFP plus empty vector (MT), p19, $P0^{CA}$, $P0^{SC}$ the photographs for the different leaf infiltrations were taken at 3 and 6 d.p.i. under UV light. (B–C and F–G) northern blots of 10 μg each of mRNA isolated from infiltrated leaves collected at 3 and 6 d.p.i. were probed with radioactively labeled GFP and $P0^{SC}$ DNA fragments. (D and H) GF and P siRNA blot analysis of 5 μg of small RNAs isolated from agro-infiltrated leaves at 3 and 6 d.p.i. fractionated on 15% PAGE–7 M Urea gel. The Hybond N+ membrane bound small RNAs were probed with a ^{32}P [α-dUTP] *in vitro*-transcribed sense GF or sense P mRNA and exposed for 2–6 h and 16 h–3 d or 2–6 h and 16 h–3 d respectively using a Phosphor Imager. In all cases equal RNA loading was checked by ethidium bromide staining of gels and photographs were taken before RNA was transferred to membranes. Lanes: 1, non-infiltrated sample (C), 2, empty vector (MT), (B) blank-no sample loaded, 3, p19, 4, $P0^{CA}$, 5, $P0^{SC}$.

cases the control sample (C) did not show any siRNAs (Figs. 3D and H, lanes 1). Unlike p19 (a suppressor that specifically binds duplex siRNAs), both $P0^{SC}$ and $P0^{CA}$, just like MT, had no effect on the levels of GF 21–24 nt primary siRNAs derived from the direct action of dicers on dsGF mRNA stem at 3 d.p.i. (RA; Fig. 3D, 2hEx/6hEx, lanes 2–5). The primary GF siRNAs require RDR6 and cofactors to produce the 3′ secondary P siRNAs from the P-region of GFP mRNA not initially targeted by dsGF, via transitivity. The P secondary siRNAs were similarly reduced in the presence of $P0^{SC}$ or $P0^{CA}$ compared to MT but not to the same extent as in p19 (RA; Fig. 3D, 16hEx/36hEx, lanes 2–5). The levels of GF primary siRNAs were higher than the P secondary siRNAs since dsGF was used to induce PTGS (Fig. 3D, compare RA; GF siRNA/2hEx/6hEx and P siRNA/16hEx/36hEx). Although $P0^{CA}$ and $P0^{SC}$ had similar amounts of both GF and P siRNAs, $P0^{CA}$ infiltrations showed GFP fluorescence that persisted beyond 6 d.p.i. (Figs. 3A and E, $P0^{CA}$ and $P0^{SC}$) and protected higher amounts of GFP mRNA (Figs. 3B, lanes 3–4 and F, lanes 4–5). Both GF and P siRNAs were also analyzed at 6 d.p.i. to determine the differences between $P0^{SC}$ and $P0^{CA}$. At 6 d.p.i., MT infiltrated leaves accumulated higher levels of 21/22–24 nt GF siRNAs than at 3 d.p.i. (compare Figs. 3D and H, 2hEx, lane 2). Interestingly both p19 and $P0^{CA}$ accumulated more of the 21/22 nt size class than the 24 nt size class, a result not seen at 3 d.p.i. (Figs. 3D and H, lanes 3–4). There was a noticeable siRNA size shift in $P0^{SC}$ infiltrated leaves from the 21 nt to the 22 nt siRNAs, whereas the 24 nt siRNAs were comparable to p19 and $P0^{CA}$ (Figs. 3D and H, compare lanes 3 and 4 with 5). The siRNAs size shift was not detectable in the GF siRNA blots analyzed from samples harvested at 3 d.p.i. The differences in siRNA accumulation were evident when the GF siRNA blots were exposed for 4 h (Fig. 3H, 4hEx).

Analysis of P siRNAs produced surprising results that may explain the differences in suppressor activity observed between $P0^{CA}$ and $P0^{SC}$. Leaves infiltrated with MT had the highest levels of 21/22 and 24 nt P siRNAs compared to p19, $P0^{CA}$ and $P0^{SC}$ (Fig. 3H, 29hEx/3dE, lanes 2 and 3–5). Both p19 and $P0^{CA}$ had reduced levels of all size classes of P siRNAs although $P0^{CA}$ clearly showed 21/22 and 24 nt sizes (Fig. 3H, 29hEx/3dEx, lanes 3 and 4). $P0^{SC}$ distinctly prevented the accumulation of the 21 nt P siRNAs while supporting high amounts of 22–24 nt siRNAs (Fig. 3H, 29hEx/3dEx, lane 5).

$P0^{SC}$ suppresses local and systemic sGFP-PTGS, and induces a cell death phenotype

PTGS in plants is divided into two forms; local and systemic (Palauqui and Vaucheret, 1998; Vaucheret et al., 1998; Voinnet et al., 1998; Voinnet, 2005). We investigated the effect of $P0^{SC}$ and deletions of $P0^{SC}$ on both local and systemic PTGS induced by sGFP in a GFP transgenic *N. benthamiana* line 16c background. Lower leaves of GFP transgenic plants were co-infiltrated with sGFP plus the respective test or control constructs. At 3 d.p.i., the initially up-regulated GFP expression in MT infiltrations had declined compared to p19, $P0^{CA}$, $P0^{SC}$ and $P0^{SC}$ deletions (Δ2, Δ2–15, Δ69–90, Δ148–256, Δ241–256 and Δ255–256) (Fig. 4A, inserts of infiltrated primary leaves under UV light). As early as 1 d.p.i., $P0^{SC}$, Δ2 and Δ255–256, unlike $P0^{CA}$, induced the characteristic cell death phenotype previously observed in wild-type *N. benthamiana* infiltrations (Fig. 4A, $P0^{SC}$, Δ2 and Δ255–256, cell death phenotype indicated by yellow arrows in inserts under normal light).

The intensity of fluorescence in the infiltrated patches correlated with the mRNA levels determined by northern blot analysis of samples harvested at 3 d.p.i. (Fig. 4B, lanes 1–11). The amount of GFP mRNA was lowest in leaves co-infiltrated with MT and Δ2–15 (Fig. 4B, lanes 1 and 6) compared to the non-infiltrated control sample (Fig. 4B, lane 11). Samples Δ69–90 and Δ148–256 had similar GFP mRNA levels as the control (Fig. 4B, lanes 7–8, and 11). GFP mRNA levels for $P0^{SC}$, Δ2, Δ241–256 and Δ255–256 co-infiltrations were significantly lower than those of p19 and $P0^{CA}$ probably reflecting the effect of cell death or differences in expression levels of p19 and $P0^{CA}$ compared to $P0^{SC}$ and its deletions (Fig. 4B, see lanes 4, 9–10 and 2–3). mRNA levels of $P0^{SC}$ and its deletions were approximately equal in the infiltrated leaves except for Δ2 and Δ148–256 that were low, whereas Δ241–256 was much stronger (Fig. 4B, P0 mRNA, lanes 4, 6–10 and 5).

The infiltrated plants were monitored under UV light for the initiation of systemic silencing in the newly emerging leaves. At 10 d.p.i., all plants infiltrated with MT, $P0^{CA}$, Δ2–15, Δ69–90, Δ148–256 and Δ241–256 showed the characteristic vein proximal GFP silencing in the new leaves (Fig. 4A). The limited systemic silencing observed in plants infiltrated with $P0^{CA}$ has not been previously reported but is probably due to low expression levels of $P0^{CA}$ protein, the effect of Ago1 on the extensive spreading of systemic silencing (Jones et al., 2006) or CABYV not infecting *N. benthamiana* (Lecoq et al., 1992) (Fig. 4A, compare $P0^{CA}$ to MT, Δ2–15, Δ69–90, Δ148–256 and Δ241–256). Interestingly, the $P0^{SC}$ and its deletions (Δ2, Δ255–256) that induced the cell death phenotype suppressed both local and systemic silencing. However, Δ241–256 that did not induce the cell death phenotype suppressed local but not systemic PTGS induced by sGFP (Fig. 4A, Δ241–256). While systemic silencing was evident in $P0^{CA}$ and Δ241–256 plants, the infiltrated leaves still strongly fluoresced (Fig. 4A, $P0^{CA}$, Δ241–256; infiltrated leaves indicated by black arrowheads). Systemic silencing was further explored by determining GFP mRNA levels in the newly emerging leaves of the infiltrated plants (Fig. 4B, lanes 12–21). MT, $P0^{CA}$, Δ2–15, Δ69–90 and Δ241–256 constructs that failed to suppress systemic silencing had reduced mRNA levels compared to the non-infiltrated control, p19, $P0^{SC}$, Δ2 and Δ255–256 (Fig. 4B, lanes 12, 14, 17–18, 20 compared to 11, 13, 15, 16 and 21). GF and P siRNAs were analyzed by northern blots to confirm PTGS (Fig. 4C). In contrast to WT *N. benthamiana* infiltrations, MT accumulated mostly 21 nt GF and P siRNAs compared to the 24 nt class (Fig. 4C, lane 1). In agreement with WT *N. benthamiana* infiltrations (Fig. 2D), p19, $P0^{CA}$, $P0^{SC}$, Δ2 and Δ255–256 drastically reduced the amount of 21–24 nt GF and P siRNAs (Fig. 4C, lanes 2–5 and 10) without completely eliminating the siRNAs (Fig. 4C, 3dEx, lanes 2–5 and 10). Deletions Δ2–15, Δ69–90 and Δ148–256, that did not suppress local and systemic PTGS preferentially accumulated higher amounts of 21 nt siRNAs than the 24 nt siRNAs compared to MT infiltrated tissues (Fig. 4C, 17hExp/3dEx/16hEx, lanes 1 and 6–8). The Δ241–256 deletion distinctly accumulated the GF and P 24 nt siRNAs instead of the 21 nt siRNAs (lane 9). The selective accumulation of the 24 nt siRNAs was particularly interesting given that Δ241–256 only suppressed local, but not systemic PTGS and also failed to induce the cell death phenotype. In all cases the non-infiltrated control did not accumulate any siRNAs (Fig. 4C, lane 11).

Fig. 4. (A) Local leaves of GFP transgenic *N. benthamiana* line 16c agro-infiltrated with sGFP plus empty vector (MT), p19, $P0^{CA}$, $P0^{SC}$, Δ2, Δ2–15, Δ69–90, Δ148–256, Δ241–256 or Δ255–256 are shown as inserted photographs taken at 3 d.p.i. under UV light. The inserted photographs taken under normal light show the cell death phenotype (yellow arrows) associated with the $P0^{SC}$, Δ2 and Δ255–256 infiltrations. Initiation of systemic PTGS was monitored under UV light and was evident at 10 d.p.i. as indicated in the photographs of whole plants showing "vein proximal GFP silencing" of distal leaves. (B) northern blot analysis of mRNA isolated from infiltrated local leaves at 3 d.p.i. and systemic leaves at 13 d.p.i. The blots were sequentially probed with radioactively labeled GFP DNA and stripped then reprobed with $P0^{SC}$. The ethidium bromide stained gel show equal RNA loading. (C) Five micrograms of total small RNAs isolated from infiltrated local leaves were fractionated on 15% PAGE–7 M Urea gel and electrotransferred to Hybond N+. The membranes were first hybridized with *in vitro*-transcribed radioactive sense GF mRNA and then stripped and hybridized with a similarly labeled sense P probe. The GF siRNA blots were exposed for 17 h–3 d and the P siRNA blot for 16 h. Equal small RNA loading is shown by the ethidium bromide stained PAGE gel photograph taken before transfer of the fractionated small RNAs to a membrane. Lanes: 1, empty vector (MT), 2, p19, 3, $P0^{CA}$, 4, $P0^{SC}$, 5–10, $P0^{SC}$ deletions (Δ2, Δ2–15, Δ69–90, Δ148–256, Δ241–256, Δ255–256), 11, GFP transgenic *N. benthamiana* line 16c, 12–21, systemic leaves of plants infiltrated as outlined for lanes 1–10.

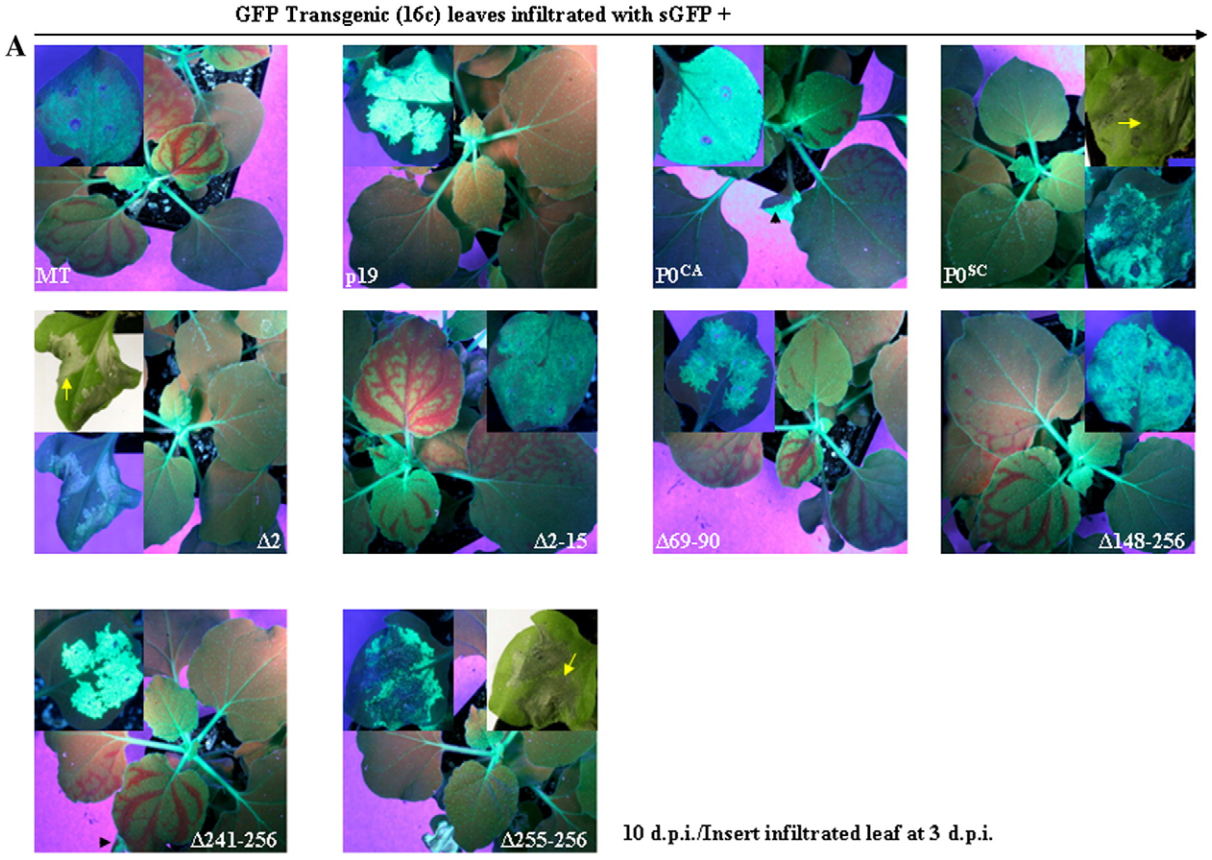
A
GFP Transgenic (16c) leaves infiltrated with sGFP +
MT
p19
P0CA
P0SC
Δ2
Δ2-15
Δ69-90
Δ148-256
Δ241-256
Δ255-256
10 d.p.i./Insert infiltrated leaf at 3 d.p.i.

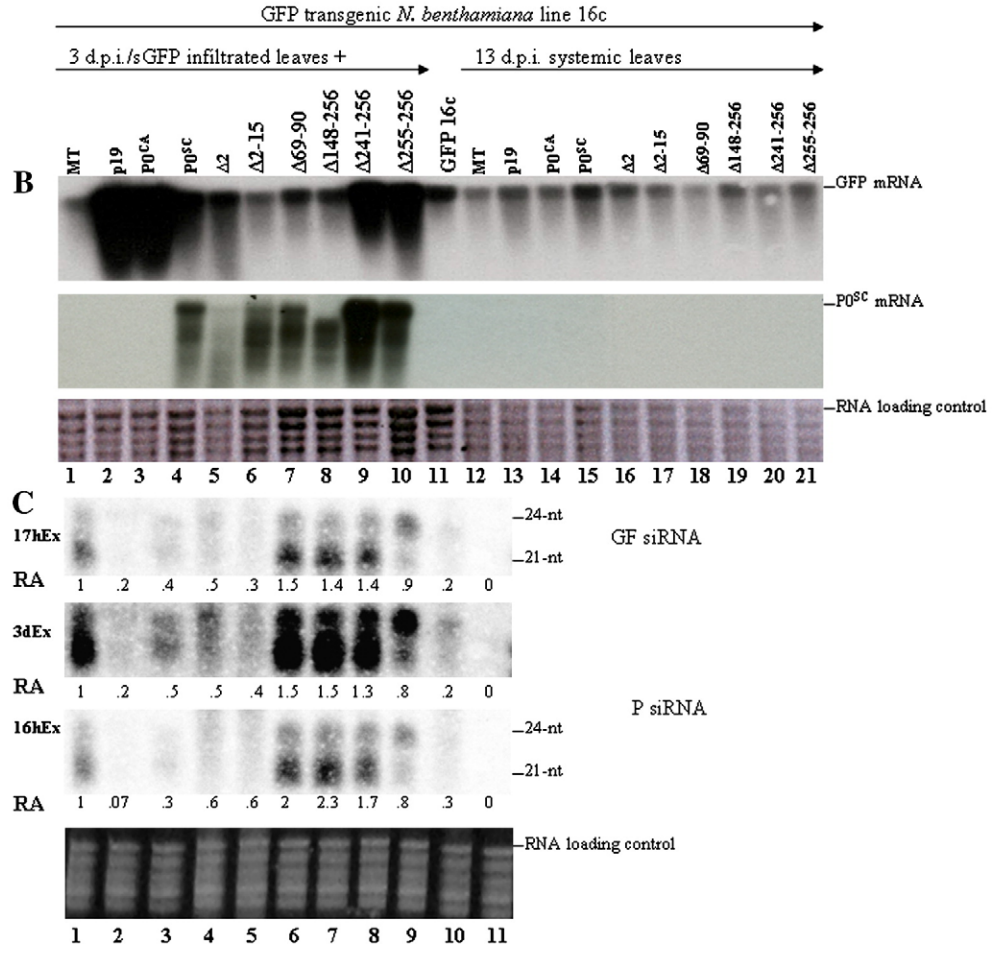
GFP transgenic N. benthamiana line 16c
3 d.p.i./sGFP infiltrated leaves +
13 d.p.i. systemic leaves
B
MT p19 P0CA P0SC Δ2 Δ2-15 Δ69-90 Δ148-256 Δ241-256 Δ255-256 GFP 16c MT p19 P0CA P0SC Δ2 Δ2-15 Δ69-90 Δ148-256 Δ241-256 Δ255-256
GFP mRNA
P0SC mRNA
RNA loading control
1 2 3 4 5 6 7 8 9 10 11 12 13 14 15 16 17 18 19 20 21
C
17hEx
RA 1 .2 .4 .5 .3 1.5 1.4 1.4 .9 .2 0
24-nt
21-nt
GF siRNA
3dEx
RA 1 .2 .5 .5 .4 1.5 1.5 1.3 .8 .2 0
16hEx
RA 1 .07 .3 .6 .6 2 2.3 1.7 .8 .3 0
P siRNA
RNA loading control
1 2 3 4 5 6 7 8 9 10 11

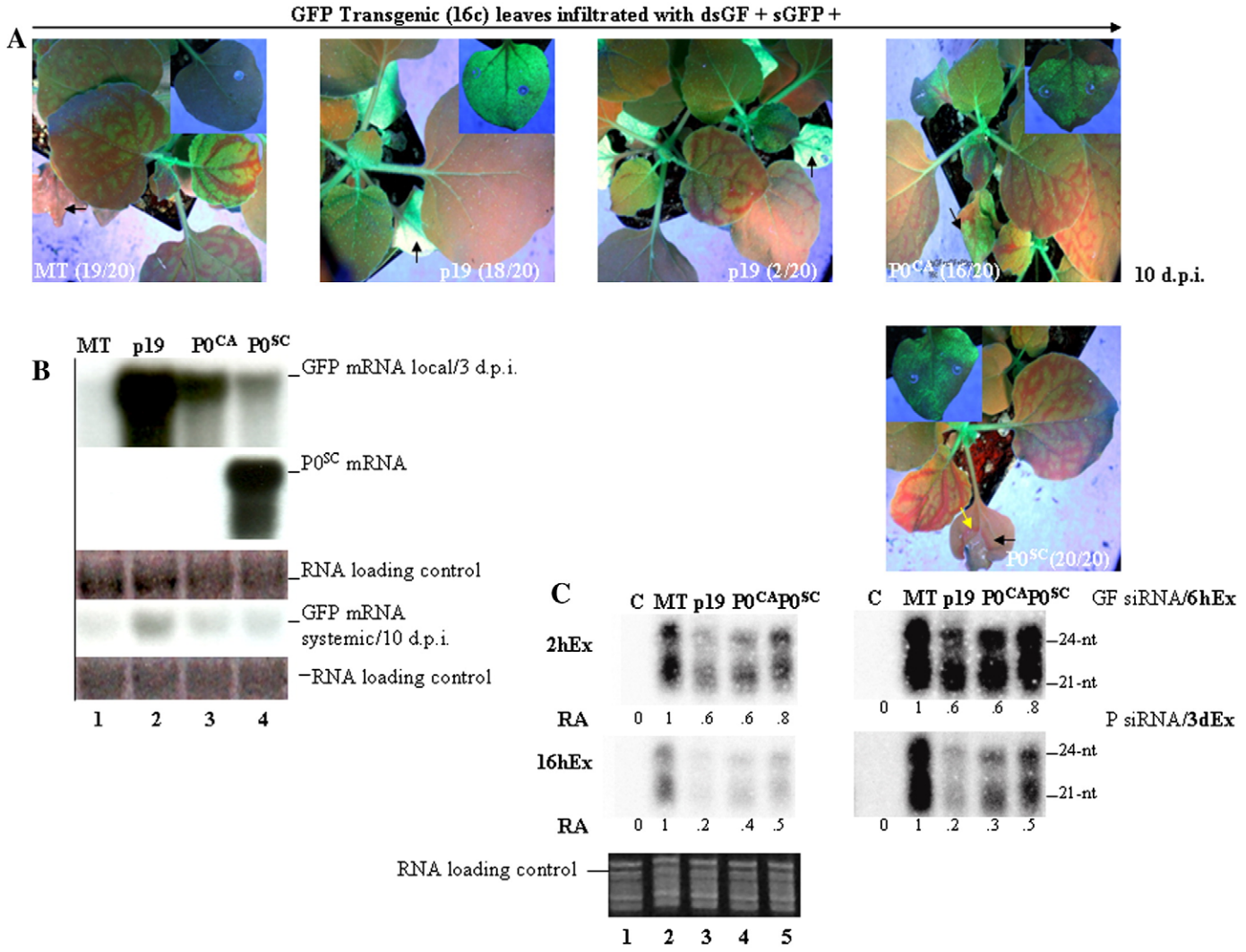

Fig. 5. (A) GFP transgenic *N. benthamiana* line 16c infiltrations of local leaves with dsGF and sGFP plus empty vector (MT), p19, $P0^{CA}$, and $P0^{SC}$ to determine the suppressor activity of $P0^{SC}$ against dsGF-PTGS. The inserted photographs of the infiltrated local leaves were taken at 3 d.p.i. under UV light. The infiltrated local leaves at 10 d.p.i. are indicated by black arrows whereas the halo ring is shown by a yellow arrow. The characteristic vein proximal GFP silencing was evident in the distal leaves of some whole plant photographs. The numbers in parentheses indicate the plants that showed systemic silencing out of total plants tested at 10 d.p.i. except for p19 that showed two phenotypes; no systemic silencing (18/20) and systemic-PTGS (2/20). (B) Northern blot analysis of 10 μg mRNA sequentially hybridized with radioactively labeled GFP and $P0^{SC}$ DNA probes was used to determine the levels of both GFP and $P0^{SC}$ mRNA from the infiltrated leaves sampled at 3 d.p.i. A GFP probe similarly labeled was used to determine GFP mRNA isolated from systemic leaves at 10 d.p.i. In all cases an ethidium bromide stained gel photograph was taken before mRNA transfer to show equal RNA loading. Lanes: 1, empty vector (MT), 2, p19, 3, $P0^{CA}$, 4, $P0^{SC}$. C, *In vitro*-transcribed sense GF and P probes were used to determine the accumulation of siRNAs from infiltrated local leaf samples. The GF siRNA blots were exposed for 2–6 h while the P siRNA blots were exposed for 16 h–3 d. Lanes: 1, non-infiltrated GFP transgenic *N. benthamiana* line 16c (C), 2, empty vector (MT), 3, p19, 4, $P0^{CA}$, 5, $P0^{SC}$.

$P0^{SC}$ does not suppress systemic dsGF-PTGS

Local leaves of GFP transgenic *N. benthamiana* line 16c co-infiltrated with dsGF and sGFP plus relevant test or control constructs were monitored under UV light for GFP fluorescence at 3 d.p.i. The leaves co-infiltrated with MT (Fig. 5A) did not show any fluorescence indicating local PTGS although the leaf had not yet turned red as seen at 10 d.p.i. (Fig. 5A, MT, insert of infiltrated leaf at 3 d.p.i. and infiltrated leaf at 10 d.p.i. shown by black arrow). The leaves infiltrated with p19 fluoresced strongly while those infiltrated with $P0^{CA}$ and $P0^{SC}$ had similar intensities at 3 d.p.i. (Fig. 5A, inserts in p19, $P0^{CA}$ and $P0^{SC}$). Interestingly, at 10 d.p.i. the leaves infiltrated with MT had turned red showing complete local PTGS while those infiltrated with $P0^{SC}$ showed the cell death phenotype surrounded by a characteristic red halo (Fig. 5A, MT and $P0^{SC}$, indicated by black and yellow arrows respectively). The red halo is indicative of short-distance cell-to-cell movement of the silencing signal also reported for $P0^{BW}$ (Baumberger et al., 2007).

The cell death phenotype was significantly delayed in this infiltration compared to sGFP plus $P0^{SC}$ (Fig. 2A, $P0^{SC}$ and Δ2 photographs taken under normal light at 3 d.p.i.). In contrast, the leaves infiltrated with p19 and $P0^{CA}$ still fluoresced strongly at 10 d.p.i. (Fig. 5A, p19 and $P0^{CA}$, infiltrated leaves indicated by black arrows). We did not observe the red halo in $P0^{CA}$ infiltrated leaves as previously reported for the related $P0^{BW}$. At 10 d.p.i., 80% or more of the plants whose primary leaves were infiltrated with empty vector, $P0^{SC}$, or $P0^{CA}$ showed prominent vein proximal GFP silencing in the newly emerging leaves (Fig. 5A, MT, $P0^{CA}$ and $P0^{SC}$, whole plant). These results show that although $P0^{CA}$ and $P0^{SC}$ both suppress local dsGF-PTGS to varying degrees, they both fail to exert the same effect on systemic PTGS. In contrast, only 10% of the plants infiltrated with p19 showed systemic dsGF-PTGS while 90% had strong GFP fluorescence in the newly emerging leaves (Fig. 5A, p19, whole plant).

The GFP fluorescence in local infiltrated leaves at 3 d.p.i. was correlated with GFP mRNA levels by northern blot analysis. GFP mRNA from MT infiltrated tissues was barely detectable which corresponded

with the weak fluorescence observed (Fig. 5B, lane 1). In contrast, leaves infiltrated with p19 that persistently showed strong fluorescence (beyond 10 d.p.i.) had the highest levels of GFP mRNA (Fig. 5B, lane 2). Although both $P0^{CA}$ and $P0^{SC}$ protected GFP mRNA, $P0^{CA}$ was more effective than $P0^{SC}$ (Fig. 5B, lanes 3–4). $P0^{SC}$ mRNA was highly expressed at 3 d.p.i. even though $P0^{SC}$ did not protect GFP mRNA as effectively as p19 and $P0^{CA}$ (Fig. 5B, lanes 2, 3 and 4). The GFP mRNA levels were also determined in the newly emerging leaves of the infiltrated plants at 10 d.p.i. The mRNA in systemic leaf tissues was very low in MT infiltrated plants although the plants showed the same phenotype as those infiltrated with $P0^{CA}$ and $P0^{SC}$ (Fig. 5B, GFP mRNA systemic/10 d.p.i., lane 1). Systemic leaves from plants infiltrated with p19 had much higher levels of mRNA compared to $P0^{CA}$ and $P0^{SC}$ (Fig. 5B, lanes 2, 3 and 4). Both $P0^{CA}$ and $P0^{SC}$ had similarly low levels of GFP mRNA that were higher than those in MT infiltrated plants.

PTGS in local leaves was confirmed by siRNA analysis of GF primary and P secondary siRNAs (Fig. 5C). The hairpin-forming dsGF effectively induced PTGS as shown by the high amounts of 21–24 nt GF siRNAs in the MT infiltrated leaves (Fig. 5C, 2hEx, lane 1). Infiltrations with p19, $P0^{CA}$, and $P0^{SC}$ accumulated 60–80% of 21–24 nt GF siRNAs compared to MT (Fig. 5C, lanes 3–5 and 2). Exposure of the siRNA blot for 6 h showed that both $P0^{SC}$ and $P0^{CA}$ had only a slight effect on the accumulation of GF siRNAs compared to the MT infiltrations (Fig. 5C, GF siRNA/6hEx). On the other hand, the RDR6-dependent P siRNAs in p19, $P0^{CA}$, and $P0^{SC}$ infiltrations accumulated 20–50% of the levels in MT infiltrated leaves (Fig. 5C, 16hEx and P siRNA/3dEx).

Cell death phenotype induced by $P0^{SC}$ is dosage dependent

We further investigated if the cell death phenotype associated with $P0^{SC}$ was dosage-dependent and whether $P0^{SC}$ lost its suppressor activity against systemic sGFP-PTGS at low concentrations. At 10 d.p.i. 100% of the plants infiltrated with sGFP plus empty vector (MT) and 50% of those infiltrated with $P0^{CA}$ and $P0^{SC}$ (1:5 dilution) were systemically silenced (Fig. 6A, and photographs not shown). In contrast, plants infiltrated with p19 and undiluted $P0^{SC}$ were not systemically silenced even after 3 weeks. At 10 d.p.i., infiltrations of sGFP plus diluted (1:5–50) $P0^{SC}$ did not induce the cell death phenotype and diluted $P0^{SC}$ progressively lost systemic-PTGS suppressing activity (50–94% of plants showed systemic silencing). Although the diluted $P0^{SC}$ failed to suppress systemic PTGS, the infiltrated primary leaves had strong GFP fluorescence indicating very strong suppressor activity against local sGFP-PTGS (results not shown). This suggests that the cell death phenotype is dependent on the concentration of $P0^{SC}$ used for infiltrations.

A

Infiltration ▼ / D.p.i. ►	6	7	10	11	12	14	17	19	21
sGFP + MT	0/15	4/15	15/15						
sGFP + p19	0/16	0/16	0/16	0/16	0/16	0/16	0/16	0/16	0/16
sGFP + $P0^{CA}$	0/16	1/16	8/16	9/16	11/16	12/16	12/16	14/16	14/16
sGFP + $P0^{SC}$	0/16	0/16	0/16	0/16	0/16	0/16	0/16	0/16	0/16
sGFP + $P0^{SC}$ (1:5)	0/16	0/16	8/16	9/16	9/16	12/16	12/16	12/16	12/16
sGFP + $P0^{SC}$ (1:10)	0/16	1/16	10/16	14/16	15/16	15/16	15/16	15/16	15/16
sGFP + $P0^{SC}$ (1:20)	0/16	2/16	14/16	15/16	15/16	15/16	16/16		
sGFP + $P0^{SC}$ (1:50)	0/16	5/16	15/16	16/16					

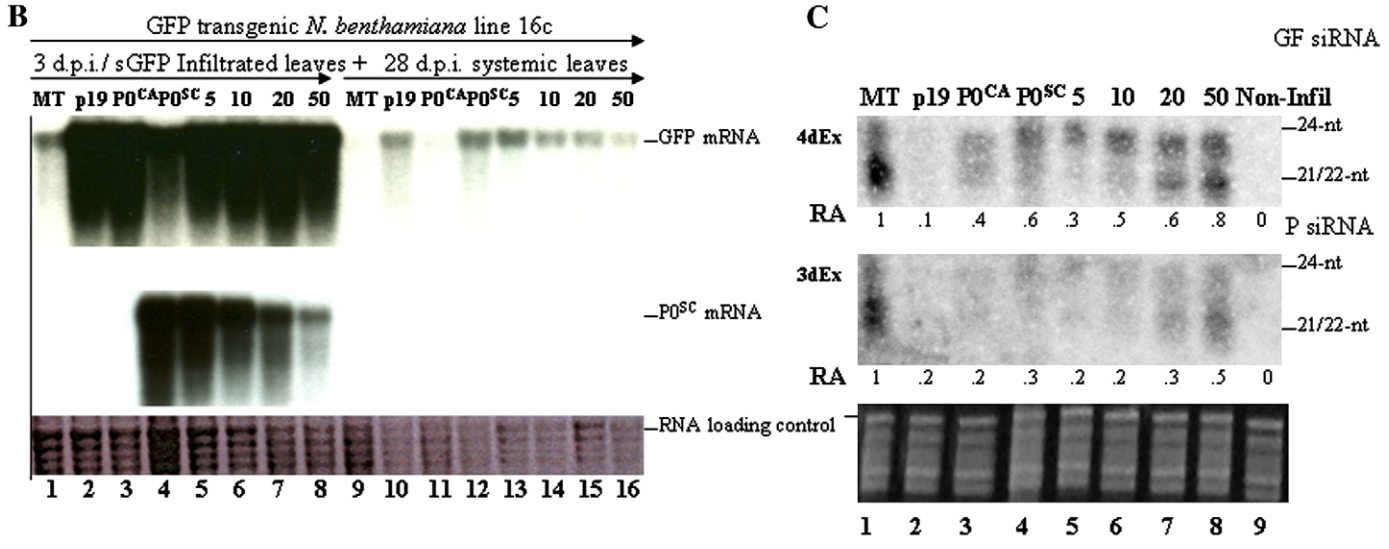

Fig. 6. (A) Dosage-dependent cell death phenotype and associated suppression of systemic sGFP-PTGS determined by infiltrating local leaves of GFP transgenic *N. benthamiana* line 16c with sGFP plus $P0^{SC}$ (undiluted), $P0^{SC}$ (1:5), $P0^{SC}$ (1:10), $P0^{SC}$ (1:20) and $P0^{SC}$ (1:50). Note that the agrobacterium strain carrying $P0^{SC}$ was serially diluted by a factor of 5, 10, 20 and 50. Systemic sGFP-PTGS was constantly monitored under UV light and results recorded for 21 d. The numbers for example 0/15, the numerator denotes the number of plants showing systemic silencing while the denominator is the total number of plants agro-infiltrated. (B) Northern analysis of mRNA isolated from local infiltrated leaves at 3 d.p.i. and systemic leaves at 28 d.p.i. was carried out using GFP and $P0^{SC}$ radioactively labeled DNA probes. (C) siRNA blots were prepared by transferring 5 μg of total small RNAs, isolated from local infiltrated leaves and fractionated on 15% PAGE–7 M Urea gel, onto Hybond N+. The membrane bound siRNAs were sequentially probed with *in vitro*-transcribed GF and P respectively. The GF and P radioactively probed blots were exposed for 4 and 3 d respectively using a Phosphor Imager. Ethidium bromide stained gels were used as RNA loading controls. Lanes: 1, empty vector (MT), 2, p19, 3, $P0^{CA}$, 4, $P0^{SC}$, 5–8, $P0^{SC}$ diluted 1:5, 1:10, 1:20 and 1:50, 9–16, same as in local leaves using systemic leaves sampled at 28 d.p.i. In C, lanes 1–8 are the same as those for northern blots in B except for lane 9 that show non-infiltrated GFP transgenic *N. benthamiana* line 16c.

Using northern blot analysis, we further explored whether the strong GFP fluorescence that we observed corresponded with the protection of mRNA by the suppressor activity of $P0^{SC}$. At 3 d.p.i., the empty vector had greatly reduced levels of GFP mRNA compared to p19, $P0^{CA}$, $P0^{SC}$ and $P0^{SC}$ dilutions (Fig. 6B, lanes 1 and 2–8). The diluted $P0^{SC}$ protected GFP mRNA more than the undiluted $P0^{SC}$ that also induced the cell death phenotype. As expected, the $P0^{SC}$ mRNA expression decreased with increasing dilution (Fig. 6B, $P0^{SC}$ mRNA panel, lanes 4–8). Importantly, regardless of the very low mRNA expression levels of $P0^{SC}$ (1:50), $P0^{SC}$ still protected high amounts of GFP mRNA (Fig. 6B, GFP mRNA and $P0^{SC}$ mRNA, lane 8). Although the diluted samples of $P0^{SC}$ effectively suppressed local sGFP-PTGS, they failed to prevent systemic silencing (Fig. 6A, 10 d.p.i.). We compared the effects of p19, $P0^{CA}$ and $P0^{SC}$ with diluted $P0^{SC}$ on GFP mRNA transcript levels in newly-emerging leaves by northern blot analysis. The diluted $P0^{SC}$ suppressed GFP mRNA silencing in a concentration dependent manner (Fig. 6B, lanes 12–16). $P0^{SC}$ (1:5 dilution) protected GFP mRNA to the same extent as p19 and undiluted $P0^{SC}$ (Fig. 6B, lanes 10, 12 and 13). $P0^{CA}$ and all diluted $P0^{SC}$ infiltrations did not induce the cell death phenotype and also failed to suppress systemic PTGS. Nevertheless, the two proteins were remarkably different in that $P0^{CA}$ at 28 d.p.i., just like MT, failed to protect GFP mRNA, whereas all the diluted $P0^{SC}$ samples had detectable GFP mRNA levels (Fig. 6B, compare lanes 9 and 11, then 9 and 11 with 13–16).

Since all the diluted $P0^{SC}$ samples suppressed local sGFP-PTGS, we determined if there were any detectable differences in the amounts of GF and P siRNAs at 3 d.p.i. The siRNA blot that was probed with GF showed a higher accumulation of 21/22-nt siRNA in tissues infiltrated with MT (Fig. 6C, lane 1; also see Fig. 4C) compared to the barely detectable levels of both size class siRNAs for p19 (lane 2). $P0^{CA}$ and $P0^{SC}$ comparably reduced the amount of both size classes of GF siRNAs (Fig. 6B, lanes 3 and 4). Intriguingly, diluted $P0^{SC}$ showed a distinct effect on GF siRNAs by accumulating relatively high amounts of the 24-nt siRNAs while the 21/22-nt siRNAs were not detected (Fig. 6C, lane 5). Increased dilutions of $P0^{SC}$ favored the reappearance of the 21/22-nt siRNAs that were not detectable in $P0^{SC}$ (1:5) (Fig. 6C, compare lanes 6–8 with 5).

The siRNA blots were stripped and reprobed with sense P mRNA to determine the levels of secondary siRNAs. Both size classes of P siRNAs were produced at very low levels in the presence of a suppressor of local PTGS (Fig. 6C, P siRNA, compare lanes 9, 1 and 2–6). Nevertheless, both size classes of P siRNAs accumulated to lower levels in infiltrations with diluted $P0^{SC}$ (1:10, 1:20, 1:50) compared to infiltrations with MT (Fig. 6C, lanes 7–8 and 1). It is important to note that for the same infiltration with mutants of $P0^{SC}$ (Δ2–15, Δ69–90 and Δ148–256; Fig. 4C, lanes 6–9) there was a distinct and equal accumulation of both GF and P siRNAs.

Discussion

SCYLV $P0^{SC}$ suppression of local sGFP-PTGS

We have demonstrated through detailed molecular analyses that $P0^{SC}$, like previously studied dicot-infecting polerovirus P0 proteins, is a strong suppressor of local sense GFP-PTGS. Sense GFP-PTGS requires RDR6 (Dalmay et al., 2000; Mourrain et al., 2000), AGO1 (Morel et al., 2002), WEX (Glazov et al., 2003), SDE3 (Dalmay et al., 2001; Himber et al., 2003) and DCL4 (Dunoyer et al., 2005; Gasciolli et al., 2005; Xie et al., 2005). PTGS is induced by dsRNA formed from over-expressed sGFP mRNA via the action of RDR6 (Curaba and Chen, 2008; Luo and Chen, 2007; Wassenegger and Krczal, 2006). The dsRNA is acted upon by RNAseIII-like dicers 2–4 but not dicer 1, (Finnegan et al., 2003) to produce 21/22–24 nt siRNAs. It is the 21–22 nt class that guides the endonucleolytic RNA induced silencing complex (RISC) to degrade target mRNA. $P0^{SC}$, like the known suppressors p19 and $P0^{CA}$, strongly up-regulate GFP expression by reducing siRNAs (Fig. 2D, lanes 2–4) thereby protecting target mRNA (Fig. 2B, lanes 2–4) from PTGS-directed degradation. $P0^{SC}$, like $P0^{CA}$ or $P0^{BW}$, specifically eliminated the 21 nt siRNAs and greatly reduced the accumulation of 22–24 nt siRNAs (Fig. 2D; Pfeffer et al., 2002). In the absence of the 21 nt siRNA producing DCL4, DCL2 produces 22 nt siRNAs that can be used as guides for GFP mRNA degradation. Both $P0^{CA}$ and $P0^{BW}$ are known to act through destabilization of Ago1 (Baumberger et al., 2007; Bortolamiol et al., 2007), a "slicer" component of the RISC complex in the PTGS pathway (Baumberger and Baulcombe, 2005). If $P0^{CA}$ and $P0^{BW}$ primarily interfere with Ago1 in sGFP-PTGS downstream of siRNA production, the levels of siRNAs in $P0^{CA}$ should be the same as in the empty vector.

The overall reduction in siRNA levels indicates that Ago1 probably acts upstream of dsRNA in sGFP-PTGS via Ago1-siRNA tagging of aberrant RNAs (including the cleavage products from AGO1 slicing activity) for RDR6-directed dsRNA formation (Brodersen and Voinnet, 2006; Wassenegger and Krczal, 2006). The results of P0 leaf infiltrations (Fig. 2D, lanes 3–4) may also indicate that $P0^{SC}$ and $P0^{CA}$ affect all of the dicers or parts of the dicer modules (Axtell et al., 2006; Brodersen and Voinnet, 2006). The $P0^{SC}$ deletions Δ2–15, Δ69–90 and Δ148–256 all reduced suppressor activity as shown by high amounts of 21–22 nt siRNAs (Fig. 2D, lanes 6–8). The 21/22 nt siRNAs are the principal guides in mRNA degradation while the 24 nt siRNAs are not involved. Our results showing selective accumulation of the 24, and to a lesser extent the 22 nt, siRNAs in Δ241–256, a deletion that has full suppressor activity (Fig. 2D, lane 9), support the hypothesis that $P0^{SC}$ preferentially interferes with DCL4 and to a lesser extent DCLs 2 and 3 or that the deletion interacts with the DCL4-specific cofactor DRB4 (Haas et al., 2008). Our deletion analysis results also indicate that the C-terminal 15 amino acid residues of $P0^{SC}$ are not required for effective suppression of sGFP-PTGS.

$P0^{SC}$, unlike $P0^{CA}$, induces a rapid cell death phenotype when transiently expressed in *N. benthamiana* leaves. Since we did not determine the mRNA levels of $P0^{CA}$, the observed differences between $P0^{SC}$ and $P0^{CA}$ may be due to different expression levels. The cell death phenotype has not been reported for previously studied P0 proteins (Pfeffer et al., 2002; Pazhouhandeh et al., 2006; Baumberger et al., 2007). However, transgenic potato plants expressing $P0^{PL}$, a weak suppressor of PTGS (Pfeffer et al., 2002), manifested severe phenotypic distortions that were similar to symptoms typical of PLRV infected plants (van der Wilk et al., 1997). Furthermore, transgenic *Arabidopsis* seedlings expressing $P0^{BW}$, a strong suppressor of PTGS that targets Ago1, failed to develop beyond the embryogenic stage. When mature $P0^{BW}$ transgenic plants produced using an estradiol-inducible XVE vector system (Bortolamiol et al., 2007) were treated with estradiol, they showed upward curling and severe crinkling of new leaves. The failure of *Arabidopsis* seedlings to develop beyond the embryogenic stage show that $P0^{BW}$ affects an early stage in plant development that is mediated by the Ago1-microRNA interaction while $P0^{PL}$ affects a later stage. The consistent pleotropic effects elicited by other polerovirus P0 proteins raise the question of whether the cell death phenotype induced by $P0^{SC}$ is a result of the interaction with both Ago1 and any of the DCLs 2–4.

The P0s of poleroviruses are generally cytopathic, however, the $P0^{SC}$ induced cell death phenotype is particularly extreme and rapid. Every $P0^{SC}$ deletion, except Δ241–256, that lost the induction of cell death phenotype also failed to suppress both local and systemic sGFP-PTGS and greatly reduced the accumulation of siRNAs (Fig. 2D, lanes 4, 5 and 10). The reduction of all siRNA size classes may be more than a non-specific effect of cell death.

Suppression of systemic sGFP-PTGS

We used GFP transgenic *N. benthamiana* line 16c to test whether $P0^{SC}$ suppresses systemic sGFP-PTGS and whether the cell death phenotype is dosage-dependent. The suppression of systemic

silencing by P0^{SC} and its deletion constructs may be due to the effects of cell death. This hypothesis is supported by infiltration with Δ241–256, a deletion that suppressed local PTGS but failed to inhibit systemic PTGS and did not induce the cell death phenotype. P0^{SC} may be blocking the movement or production of the systemic signal because of factors involved in cell death.

The siRNA accumulation in sGFP-PTGS in a GFP transgenic background differed from that in WT *N. benthamiana* in that the former preferentially accumulated the DCL4-dependent 21 nt size class while the latter accumulated all sizes at similar levels (Figs. 4C and 2D, lane 1). The preferential accumulation of the 21 nt siRNAs suggests that DCL4 is the major dsRNA cleaving enzyme, an observation that was previously noted in IR-PTGS (Brodersen and Voinnet, 2006; Gasciolli et al., 2005; Fusaro et al., 2006; Liu et al., 2007). Although no specific siRNAs have been identified as being responsible for systemic silencing signaling (Hamilton et al., 2002; Mallory et al., 2001; Mlotshwa et al., 2002; Brosnan et al., 2007; Dunoyer and Voinnet, 2008), the accumulation of the 24 nt siRNA in P0^{SC} Δ241–256 points to a possible role of this siRNA species.

The cell death phenotype is dependent on the dosage of P0^{SC}, but P0^{SC} dilutions did not affect the suppressor activity against local sGFP-PTGS (Fig. 6B). In fact, diluted P0^{SC} protected increased levels of GFP mRNA by effectively reducing the 21–22 nt siRNAs (Fig. 6C, lanes 5–6) perhaps by mitigating cytopathic effects. P0^{SC} prevented the accumulation of DCL2 and DCL4-dependent 21–22 nt siRNAs in a dosage-dependent manner (Fig. 6C, lanes 5–8) in an agro-infiltration system that preferentially favors DCL4 to act on RDR6-produced GFP dsRNA. However, diluted P0^{SC} failed to suppress systemic silencing (Fig. 6A). Because we only diluted P0^{SC} and not sGFP or the combination of sGFP and P0^{SC} in co-infiltrations as previously reported for *Tobacco rattle virus* (TRV)-encoded 16-kDa suppressor (Martínez-Priego et al., 2008), we cannot conclude that the cell death phenotype is responsible for the suppression of systemic sGFP-PTGS. Furthermore, the plants that were infiltrated with the non-cell death inducing P0^{SC} dilutions, but not P0^{CA} or MT, showed GFP mRNA protection in systemic leaves that were sampled at 28 d.p.i. The suppression conferred by a P0^{SC} (1:5) dilution, as shown in Fig. 6B (lanes 10 and 13) was equivalent to that of p19, a known strong suppressor of systemic sGFP-PTGS.

Suppression of local and systemic dsGF-PTGS

dsGF-PTGS can occur in *rdr*6, *sgs*3 and *ago*1 mutants (Beclin et al., 2002) by direct action of DCLs 2, 3 and 4 on hairpin RNAs (Fusaro et al., 2006). We tested whether P0^{SC} suppressed PTGS induced by dsGF that precluded RDR6-dependent dsRNA in both WT and GFP transgenic *N. benthamiana* backgrounds. P0^{CA} reduced the levels and did not affect the size of secondary P siRNAs as previously reported (Baumberger et al., 2007; Bortolamiol et al., 2007), but we clearly observed the 21, 22 and 24 nt siRNAs (Liu et al., 2007; Mette et al., 2000; Fig. 3H, 29hEx/3dEx, lane 4). In contrast, the presence of P0^{SC} abolished the accumulation of the RDR6-dependent DCL4 specific 21 nt siRNAs (Fig. 3H, 29hEx/3dEx, lane 5). This result strongly suggests that P0^{SC} targets DCL4, or an RDR6/DCL4 module, leaving DCLs 2 and 3 to produce the 22–24 nt secondary siRNAs from GFP. This result is equivalent to GUS transgenic *Arabidopsis dcl*4 mutants transformed with ΔGUS–SUG (Mlotshwa et al., 2008) and previous reports (Fusaro et al., 2006; Moissiard et al., 2007; Liu et al., 2007). The limited P0^{SC} suppressor activity against local dsGF-PTGS suggests that DCL4 is important, but not essential, for this type of silencing, which is also consistent with previous reports (Fusaro et al., 2006). In GFP transgenic *N. benthamiana*, both P0^{SC} and P0^{CA} suppressed local, but not systemic, dsGF-PTGS (Figs. 5A and B, lanes 3–4). P0^{SC} plants showed the characteristic red fluorescent halo ring surrounding the infiltrated leaf, which is characteristic of the cell-to-cell movement of the silencing signal.

Mode of P0^{SC} action

The P0^{CA} and P0^{BW} both targeted destruction of Ago1 protein, which is consistent with suppression of local, but not systemic PTGS. Because siRNA production is upstream of Ago1-RISC complex, loss of Ago1 activity should not interfere with the production of siRNAs that may act as the systemic signal of PTGS. Instead, loss of Ago1 prevents the formation of an active RISC complex that is required for target mRNA cleavage and also limit the extent of systemic silencing (Jones et al., 2006). Since P0^{SC} did suppress systemic PTGS (triggered by sGFP), it presumably has a different or additional modes of action, from other P0s. This hypothesis is supported by the reduced levels of siRNAs produced in response to P0^{SC} expression. Curiously, P0^{CA} and P0^{BW} block the accumulation of siRNAs generated in response to a sGFP trigger (this paper; Pazhouhandeh et al., 2006; Pfeffer et al., 2002), but siRNAs accumulate abundantly when PTGS is triggered by a dsRNA hairpin (Baumberger et al., 2007; Bortolamiol et al., 2007). These differences in levels of siRNAs suggest that Ago1, in addition to its "slicer" activity, has some role in siRNA production from sRNA templates, but not from dsRNA templates. Alternatively, P0^{CA} and P0^{BW} may have an activity that suppresses siRNA production from an aberrant mRNA template in addition to destroying Ago1 activity. We conclude that P0^{SC} from a monocot-infecting virus targets DCL4 and clearly differs functionally from previously characterized P0 proteins. Future research will further characterize these differences, especially the rapid cell death phenotype, since DCL4 and Ago1 play a critical role in developmental timing and specifying adaxial/abaxial identities of the leaf (Liu et al., 2007; Adenot et al., 2006; Gasciolli et al., 2005; Garcia et al., 2006; Yang et al., 2006).

Materials and methods

Plant materials and growth conditions

WT and GFP transgenic *N. benthamiana* plants were grown at 25 °C under 12 h illumination at 2000 lm m^{-2} (34 W fluorescent bulbs). The GFP transgenic *N. benthamiana* line 16c which contains a single copy of pBin-35S-mGFP5 (mGFP; GenBank accession no. U70495.1; Haseloff et al., 1997; Siemering et al., 1996) was a generous gift from Dr. David Baulcombe.

Constructs

Binary plasmids containing sGFP (pBICGFP), dsGFP (inverted repeats; pBICdsGFP), and TBSV p19 (pBICp19), all under the control of the CaMV 35S promoter (Takeda et al., 2002) and used in *N. benthamiana* leaf infiltration experiments with *Agrobacterium*, were obtained as generous gifts from Dr. Kazuyuki Mise. The GFP gene used in pBICGFP and pBICdsGFP is "smGFP" a modified version of mGFP5 (Davis and Vierstra, 1998). The smGFP has 90% overall nucleotide sequence identity with the stably integrated GFP gene (mGFP5) in line 16c; the two GFP genes share 3 regions of greater than 150 bp each with 100% identity. All the PCR amplifications for expression constructs in this paper were performed with Phusion DNA polymerase kit (Finnzymes). P0^{SC}, UTP0 (untranslatable; start codon ATG replaced by stop codon TGA) and P0 deletion constructs were PCR amplified from plasmid pFM262 (Moonan et al., 2000) using primers (see Table 1 for primer sequences) with 5′ BglII and 3′ SalI restriction sites and cloned into the TA vector pCRIITOPO (Invitrogen). The P0^{SC}, UTP0 and deletion fragments were cloned from BglII–SalI digests of pCRIITOPO into corresponding sites of a binary plasmid pGD that uses the CaMV 35S promoter (Goodin et al., 2002). The resulting constructs were designated pGDP0, pGDUTP0 and pGDP0Δ (relevant amino acids deleted for example; 69–90). pGD was used as the "empty vector" control in all the infiltration experiments. The internal deletion construct, P0Δ69–90, was made by PCR amplification of the entire

Table 1
Primers used for PCR amplification of genes used to make expression constructs and siRNAs oligo size markers

Primer	Sequence
BglIIP0F	agatctATGCTTTTCAACGAATTC
BglIIP0UTF	TCGAagatctGACTTTTCACCGAATTCTCTGT
BglIIP0(2)F	ggtaacatctATGTTCAACGAATTCTCTGTT
BglIIP0(15)F	ggtaagatcgatgCACGAAAGCACTTCACC
BglIIP0(30)F	ggtaagatcgatgTTGACCTACTACAGAGTCTT
BglIIP0(69)F	GACagatctATGCTGGAGCACATTCGCCTTAT
BglIIP0(91)F	GACagatctATGGGACGGCACATCCATTCCATATTAAG
BglIIP0(126)F	agatctATGGTACTCGAGCAAGATC
BglIIP0(136)F	agatctATGCTTTTCCGAACTCAGCT
BglIIP0(148)F	agatctATGGATGTTTTTCAAGATG
SalIP0R	CGTAgtcgacCTATATATCATGAGAATAGGTG
SalIP0(256)R	agctgtcgacctaATCATGAGAATAGGTGCTAC
SalIP0(255)R	agctgtcgacctaATGAGAATAGGTGCTACGAC
SalIP0(241)R	agctgtcgacctaCTCATTAGGTGGTAGACCAT
SalIP0(226)R	agctgtcgacctaATTATCAAAATCGGTTTCCA
SalIP0(212)R	CGAgtcgacGATGTCATCGTCATGATCAAGCG
SalIP0(147)R	gtcgacCAACCCAGCATACTGGAGT
SalIP0(90)R	gtcgacTCCAATGGTTGTGTCTGGC
SalIP0(68)R	gtcgacCCAGTTGTAAACGGGAGTG
TMDP0(69)R	p-CCAGTTGTAAACGGGAGTGTTGGGG
TMDP0(91)F	p-CGGCACATCCATCCATATTAAGAGACAGT
GF5	CACTGGAGTTGTCCCAATTC
GF3	CTTCAGCACGTGTCTTGTAG
P5	CAACAGGATCGAGCTTAAGG
P3	GTAATCCCAGCAGCTGTTAC
GF25nt	GCCCATTAACATCACCATCTAATTC
GF23nt	TTGTGCCCATTAACATCACCATC
GF21nt	TCCGTATGTTGCATCACCTTC
P24nt	GTCTGCTAGTTGAACGCTTCCATC
P22nt	TTCCAACTTGTGGCCGAGGATG
P21nt	CCCTTAAGCTCGATCCTGTTG

Lower case nucleotides indicate modifications added to facilitate cloning, *p* indicates 5′ phosphorylation, F and R represent forward and reverse primers respectively and UT, untranslatable.

pGDP0 plasmid with 5′-phosphorylated abutting primers starting from residues 68 and 91 respectively. The PCR product was circularized by blunt end-ligation and digested with DpnI to remove any residual parental plasmid before transformation into competent Top10 *E. coli* cells (Invitrogen).

For construction of dsGF, a GF fragment was amplified from pBICGFP (Takeda et al., 2002) using the GF5 and GF3 primers (Table 1) and cloned into pCR8 (Invitrogen, Inc.). Orientation of the fragment with respect to the attL1 and attL2 sites on pCR8 was verified by digestion with enzymes NdeI and XbaI. The GF fragment in the 5′ to 3′ orientation (pML401) was cloned into pHellsgate8 (Helliwell and Waterhouse, 2003) using LR Clonase™ (Invitrogen, Inc.). The clone with the GF fragment in the reverse orientation in pCR8 (pML402) was used for the GF probe preparation. The P fragment was PCR amplified using primers P5 and P3 (Table 1) and cloned in pCR8 as for the GF fragment. The plasmid was designated pML403. All constructs, except pGDP0Δ1–91 which has a silent G to A mutation at nucleotide position 229 of the $P0^{SC}$ ORF, were confirmed correct by sequencing (University of Hawaii Biotechnology—Molecular Biology Instrumentation Facility).

Agro-infiltration

Agrobacterium tumefaciens C58C1 (Ti plasmid pCH32), a gift from Dr. David Baulcombe, was transformed with relevant plasmids using the freeze–thaw method (Hofgen and Willmitzer, 1988). From here on, the agrobacterium culture will be referred to using the name of the protein expressed by the plasmid that was used to transform competent agrobacterium cells. Infiltrations into *N. benthamiana* leaves were carried out as previously described (Llave et al., 2000). Briefly, a 5 ml overnight culture of *A. tumefaciens* C58C1 harboring a relevant binary plasmid was inoculated into 50 ml of LB supplemented with 50 μg/ml kanamycin, 5 μg/ml tetracycline and 20 μM acetosyringone. The culture was incubated at 28 °C for 16 h. Agrobacterium cells were pelleted at 5000 rpm for 10 min and resuspended to an OD_{600} of 0.5 in infiltration medium (Llave et al., 2000). The cells were incubated at room temperature for 3 h before infiltration. For a given experiment, different agrobacterium mixtures of equal volumes and the same optical densities were used.

GFP imaging

Plants were illuminated with two 100 W ultraviolet (long wavelength 365 nm) lamps (Spectroline model SB-100P). Images were captured with an EOS 10D camera (Canon) and processed using Microsoft Office Image Manager software.

Total RNA isolation for northern blot analysis

Approximately 2–3 g of frozen fresh samples of infiltrated leaves were ground to a fine powder in liquid nitrogen and transferred to 50 ml sorval tubes. Six milliliters of HCL–Tris saturated phenol were added and the tubes were vortexed to mix well before adding 12 ml of TENS buffer (100 mM NaCl, 10 mM Tris–HCL, 1 mM EDTA and 1% SDS). The well mixed contents were incubated at 70 °C for 5 min and 5.6 ml of chloroform was added and vortexed for 1 min. The tubes were spun at 10 000 rpm for 10 min and 10 ml of the upper aqueous phase was transferred to a new 50 ml tube. A 1:10 volume of 3 M sodium acetate (pH 5.2) and 3 volumes of 100% ethanol were added to the aqueous supernatant. The contents were gently mixed and incubated for 2 h at −20 °C.

The tubes were spun at 10 000 rpm for 10 min, the supernatant was discarded and the pellet was washed with 5 ml of 70% ethanol. The tubes were spun at 3000 rpm for 5 min and the 70% ethanol was removed. The pellet was air dried and resuspended in 200–400 μl of DEPC treated water. The RNA samples were transferred to eppendorf tubes and the concentration was determined by a spectrophotometer.

Northern blot analysis

Ten micrograms of high molecular weight RNA isolated from agrobacterium infiltrated leaves was mixed with 7 μl of RNA cooker (5 ml deionized formamide, 1.62 ml 37% formaldehyde, 0.4 ml 500 mM HEPES (pH 7.5), 0.02 ml 500 mM EDTA (pH 7.5), and 2.96 ml sterile DEPC treated water) and incubated at 65 °C for 4 min. The sample was transferred to ice and 2 μl of bromophenol blue loading buffer was added. The RNA samples were fractionated on a 1.6% formaldehyde-agarose gel in HEPES buffer run at 60 V for 2 h. The gel was stained in HEPES buffer containing ethidium bromide and photographs were taken. Downward blotting was set up to transfer mRNA to Hybond-XL membranes (Amersham GE Healthcare) using 20×SSC for 16 h. Thereafter the membrane was heat treated at 80 °C for 10 min and UV crosslinked at 1200 μJ×100. The membrane was again heat treated at 80 °C for 2 h and stored at room temperature until used.

The membrane was briefly washed in 5×SSC for 1 min at room temperature. The wash solution was discarded and enough Church's buffer was added to prehybridize the membrane at 65 °C for 2–16 h. Two DNA probes, GFP and $P0^{SC}$, were prepared according to instructions in the Random Prime Labeling kit (Invitrogen) using radioactive ^{32}P-[dCTP] (Perkin Elmer). Briefly, 25 μl (100–500 ng) each of GFP and $P0^{SC}$ DNA fragments were boiled, incubated on ice and random prime mix (2 μl each of dATP, dGTP, dTTP and 15 μl random primers buffer mix, 5 μl of ^{32}P [α-dCTP], 1 μl of Klenow Fragment mixed thoroughly by pippeting up and down) were added to an eppendorf tube. The mixture was incubated at room temperature for 2–3 h. The reaction was stopped by adding 5 μl of stop buffer. Unincorporated radioactive nucleotides were retained in a Sephadex

G50 column (Sigma) and the labeled DNA probe was collected in eppendorf tubes. The probe was boiled for 5 min, added to Church's buffer/membrane and incubated for 16 h at 65 °C. The membranes were washed three times as follows: 2×SSC+0.5% SDS at 65 °C for 20 min, 1×SSC+0.25% SDS at 65 °C for 20 min and lastly 0.5×SSC+0.125% SDS at 65 °C for 20 min. The membrane was covered in saran wrap and excess wash buffer removed before exposure to X-ray film for 30 min–16 h.

Total RNA extraction for siRNA blots

Leaves were flash frozen in liquid nitrogen immediately after harvest and stored at −80 °C until processed. Approximately 100 mg of frozen leaf tissue was ground with mortar and pestle, under liquid nitrogen, to a fine powder. High and low molecular weight RNAs were isolated together following instructions in the *mir*Vana™ miRNA isolation kit (Ambion, Inc., USA). Total RNA was recovered in 100 µl of 0.1 mM EDTA (pH 8.0) and stored at −80 °C until used. The concentration was determined by spectrophotometry.

siRNA northern hybridizations

To analyze siRNAs, 5 µg of total RNA from infiltrated leaves were fractionated on a 15% denaturing polyacrylamide–7 M urea gel in 1X Tris–borate–EDTA (TBE) buffer. Mixtures of 250 pg each of 21, 23, 25 nt GF and 21, 22, 25 nt P DNA oligonucleotides were run as size markers (Table 1). Following electrophoresis, RNAs were visualized by staining in ethidium bromide (0.5 µg/ml in 1× TBE buffer) and photographed. The RNA was transferred to Hybond N+ membranes (GE Healthcare, Inc., USA) by electroblotting in 0.5× TBE at 500 mA for 1 h. The transferred RNA was UV crosslinked to the membrane at 1200 µJ in a UV Stratalinker 1800 (Stratagene). Membranes were stored at 4 °C until probed. Radioactive probes were prepared from cloned fragments of GFP ligated into plasmid vector pCR8. 32P-labelled RNA transcripts were produced from 1 µg of linearized vector pCR8-GF or P (pML402 and pML403) using Maxiscript™ in-vitro transcription kits (Ambion, Inc.) according to the manufacture's protocol. For effective siRNA hybridization, the sense GF and P probes were partially hydrolyzed in sodium carbonate buffer (120 mM Na_2CO_3; 80 mM $NaHCO_3$) at 60 °C for 3 h and neutralized with 3 M sodium acetate (pH 5.2) before use. The membranes were pre-hybridized in Ultrahybe-oligo™ (Ambion, Inc.) for 1–3 h at 40 °C. After addition of the RNA probe, hybridization was performed at 40 °C overnight. Following hybridization, the membranes were washed 3 times in 2×SSC+0.2% SDS 40 °C and blots were analyzed on a GS-505 Molecular Imager System (BioRad, Inc.). The total band intensities of both size classes of siRNAs in individual lanes were normalized against the band intensities of the control sample (MT) and used to determine the relative abundance (RA) of siRNAs. The membranes were reprobed once after stripping them in 0.1% SDS at 95 °C.

Acknowledgments

We thank Jim Carr, Eva Ahrendt, Triton Peltier and Joe Molina for excellent technical work. This work was partially supported by a cooperative agreement (No. CA 58-3020-8-134) between USDA-ARS and HARC, and in part by a grant from the USDA-CSREES Tropical/Subtropical Agricultural Research (Award No. 2005-34135-16381).

References

Abu Ahmad, Y., Rassaby, L., Royer, M., Borg, Z., Braothwaite, K.S., Mirkov, T.E., Irey, M.S., Perrier, X., Smith, G.R., Rott, P., 2006. Yellow leaf of sugarcane is caused by at least three different genotypes of sugarcane yellow leaf virus, one of which predominates on the Island of Réunion. Arch. Virol. 151, 1355–1371.

Adenot, X., Elmayan, T., Lauressergues, D., Boutet, S., Bouché, N., Gascioli, V., Vaucheret, H., 2006. DRB4-dependent *TAS3 trans*-acting siRNAs control leaf morphology through AGO7. Curr. Biol. 16, 927–932.

Axtell, M.J., Jan, C., Rajagopalan, R., Bartel, D.P., 2006. A two-hit trigger for siRNA biogenesis in plants. Cell 127, 565–577.

Baumberger, N., Baulcombe, D., 2005. *Arabidopsis* ARGONAUTE1 is an RNA slicer that selectively recruits microRNAs and short interfering RNAs. Proc. Natl. Acad. Sci. U. S. A. 102, 11928–11933.

Baumberger, N., Tsai, C.H., Lie, M., Havecker, E., Baulcombe, D., 2007. The polerovirus silencing suppressor P0 targets ARGONAUTE proteins for degradation. Curr. Biol. 17, 1609–1614.

Beclin, C., Boutet, S.V., Waterhouse, P., Vaucheret, H., 2002. A branched pathway for transgene-induced RNA silencing in plants. Curr. Biol. 12, 684–688.

Borth, W., Hu, J.S., Schenck, S., 1994. Double-stranded RNA associated with sugarcane yellow leaf syndrome. Sugar Cane 3, 5–8.

Bortolamiol, D., Pazhouhandeh, M., Marocco, K., Genschick, P., Ziegler-Graff, V., 2007. The polerovirus F Box protein P0 target ARGONAUTE1 to suppress RNA silencing. Curr. Biol. 17, 1615–1621.

Boutet, S., Vazquez, F., Liu, J., Beclin, C., Fargard, M., Gratias, A., Morel, J.B., Crete, P., Chen, X., Vaucheret, H., 2003. *Arabidopsis HEN1*: a genetic link between endogenous miRNA controlling development and siRNA controlling transgene silencing and virus resistance. Curr. Biol. 13, 843–848.

Brodersen, P., Voinnet, O., 2006. The diversity of RNA silencing pathways in plants. Trends Genet 22, 268–280.

Brosnan, C.A., Mitter, N., Christie, M., Smith, N.A., Waterhouse, P.M., Carroll, B.J., 2007. Nuclear gene silencing directs reception of long-distance mRNA silencing in *Arabidopsis*. Proc. Natl. Acad. Sci. U. S. A. 104, 14741–14746.

Comstock, J.C., Irey, M.S., Lockhart, B.E.L., Wang, Z.K., 1998. Incidence of yellow leaf syndrome in CP cultivars based on polymerase chain reaction and serological techniques. Sugar Cane 4, 21–24.

Curaba, J., Chen, X., 2008. Biochemical activities of *Arabidopsis* RNA-dependent RNA polymerase 6. J. Biol. Chem. 283, 3059–3066.

Dalmay, T., Hamilton, A., Rudd, S., Angell, S., Baulcombe, D.C., 2000. An RNA-dependent RNA polymerase gene in *Arabidopsis* is required for posttranscriptional gene silencing mediated by a transgene but not by a virus. Cell 101, 543–553.

Dalmay, T., Horsefield, R., Braunstein, T.H., Baulcombe, D.C., 2001. SDE3 encodes an RNA helicase required for post-transcriptional gene silencing in *Arabidopsis*. EMBO J. 20, 2069–2077.

Davis, S.J., Vierstra, R.D., 1998. Soluble, highly fluorescent variants of green fluorescent protein (GFP) for use in higher plants. Plant Mol. Biol. 36, 521–528.

Dunoyer, P., Voinnet, O., 2008. Mixing and matching: the essence of plant systemic silencing? Trends Genet 24, 151–154.

Dunoyer, P., Himber, C., Voinnet, O., 2005. DICER-LIKE 4 is required for RNA interference and produces the 21-nucleotide small interfering RNA component of the plant cell-to-cell silencing signal. Nat. Genet. 37, 1356–1360.

Finnegan, E.J., Margis, R., Waterhouse, P.M., 2003. Posttranscriptional gene silencing is not compromised in the *Arabidopsis* CARPEL FACTORY (DICER-LIKE1) mutant, a homolog of Dicer-1 from *Drosophila*. Curr. Biol. 13, 236–240.

Fusaro, A.F., Matthew, L., Smith, N.A., Curtin, S.J., Dedic-Hagan, J., Ellacott, G.A., Watson, J.M., Wang, M.B., Brosnan, C., Carroll, B.J., Waterhouse, P.M., 2006. RNA interference-inducing hairpin RNAs in plants act through the viral defence pathway. EMBO Rep. 7, 1168–1175.

Garcia, D., Collier, S.A., Byrne, M.E., Martienssen, R.A., 2006. Specification of leaf polarity in *Arabidopsis* via the trans-acting siRNA pathway. Curr. Biol. 16, 933–938.

Gascioli, V., Mallory, A.C., Bartel, D.P., Vaucheret, H., 2005. Partially redundant functions of *Arabidopsis* DICER-like enzymes and a role for DCL4 in producing trans-acting siRNAs. Curr. Biol. 15, 1494–1500.

Glazov, E., Phillips, K., Budzizewski, G.J., Schob, H., Meins Jr., F., Levin, J.Z., 2003. A gene encoding an RNase D exonuclease-like protein is required for post-transcriptional silencing in *Arabidopsis*. Plant J. 35, 342–349 Erratum in. Plant J. 36, 741.

Goodin, M.M., Dietzgen, R.G., Schichnes, D., Ruzin, S., Jackson, A.O., 2002. pGD vectors: versatile tools for the expression of green and red fluorescent protein fusions in agroinfiltrated plant leaves. Plant J. 31, 375–383.

Haas, G., Azevedo, J., Moissiard, G., Geldreich, A., Himber, C., Bureau, M., Fukuhara, T., Keller, M., Voinnet, O., 2008. Nuclear import of CaMV P6 is required for infection and suppression of the RNA silencing factor DRB4. EMBO J. advance online publication 1doi:10.1038/emboj.2008.129.

Hamilton, A., Baulcombe, D., 1999. A species of small antisense RNA in posttranscriptional gene silencing in plants. Science 286, 950–952.

Hamilton, A., Voinnet, O., Chappell, L., Baulcombe, D., 2002. Two classes of short interfering RNA in RNA silencing. EMBO J. 21, 4671–4679.

Haseloff, J., Siemering, K.R., Prasher, D.C., Hodge, S., 1997. Removal of a cryptic intron and subcellular localization of green fluorescent protein are required to mark transgenic *Arabidopsis* plants brightly. Proc. Natl. Acad. Sci. U. S. A. 94, 2122–2127.

Helliwell, C., Waterhouse, P., 2003. Constructs and methods for high-throughput gene silencing in plants. Methods 30, 289–295.

Himber, C., Dunoyer, P., Moissiard, C., Ritzenthaler, C., Voinnet, O., 2003. Transitivity-dependent and -independent cell-to-cell movement of RNA silencing. EMBO J. 22, 4523–4533.

Hofgen, R., Willmitzer, L., 1988. Storage of competent cells for Agrobacterium transformation. Nucleic Acids Res. 16, 9877.

Johansen, L.K., Carrington, J.C., 2001. Silencing on the spot. Induction and suppression of RNA silencing in the Agrobacterium-mediated transient expression system. Plant Physiol. 126, 930–938.

Jones, L., Keining, T., Eamens, A., Vaistij, F.E., 2006. Virus-induced gene silencing of *Argonaute* genes in *Nicotiana benthamiana* demonstrates that extensive systemic silencing requires *Argonaute1*-like and *Argonaute4*-like genes. Plant Physiol. 141, 598–606.

Lecoq, H., Bourdin, D., Wipfscheibe, L.C., Bon, M., Lot, H., Lemaire, O., Herrbach, E., 1992. A new yellowing disease of cucurbits caused by a luteovirus, cucurbit aphid-borne yellows virus. Plant Pathol. 41, 749–761.

Liu, B., Chen, Z., Song, X., Liu, C., Cui, X., Zhao, X., Fang, J., Xu, W., Zhang, H., Wang, X., Chu, C., Deng, X., Xue, Y., Cao, X., 2007. Oryza sativa Dicer-like4 reveals a key role for small interfering RNA in plant development. Plant Cell 19, 2705–2718.

Llave, C., Kasschau, K.D., Carrington, J.C., 2000. Virus-encoded suppressor of posttranscriptional gene silencing targets a maintenance step in the silencing pathway. Proc. Natl. Acad. Sci. U. S. A. 97, 13401–13406.

Luo, Z., Chen, Z., 2007. Improperly terminated, unpolyadenylated mRNA of sense transgenes is targeted by RDR6-mediated RNA silencing in *Arabidopsis*. Plant Cell 19, 943–958.

Mallory, A.C., Ely, L., Smith, T.H., Marathe, R., Anandalakshmi, R., Fagard, M., Vaucheret, H., Pruss, G., Bowman, L., Vance, V.B., 2001. HC-Pro suppression of transgene silencing eliminates the small RNAs but not transgene methylation or the mobile signal. Plant Cell 13, 571–583.

Martínez-Priego, L., Donaire, L., Barajas, D., Llave, C., 2008. Silencing suppressor activity of the *Tobacco rattle virus*-encoded 16-kDa protein and interference with endogenous small RNA-guided regulatory pathways. Virology 376, 346–356.

Mette, M.F., Aufsatz, W., van der Winden, J., Matzke, M.A., Matzke, A.J.M., 2000. Transcriptional silencing and promoter methylation triggered by double-stranded RNA. EMBO J. 19, 5194–5201.

Mlotshwa, S., Voinnet, O., Mette, M.F., Matzke, M., Vaucheret, H., Ding, S.W., Pruss, G., Vance, V.B., 2002. RNA silencing and the mobile silencing signal. Plant Cell 14, S289–S301.

Mlotshwa, S., Pruss, G.J., Peragine, A., Endres, M.W., Li, J., Chen, X., Poethig, R.S., Bowman, L.H., Vance, V., 2008. *DICER-LIKE2* plays a primary role in transitive silencing of transgenes in *Arabidopsis*. PLoS One 3, e1755.

Moissiard, G., Parizotto, E.A., Himber, C., Voinnet, O., 2007. Transitivity in *Arabidopsis* can be primed, requires the redundant action of the antiviral Dicer-like 4 and Dicer-like 2, and is compromised by viral-encoded suppressor proteins. RNA 13, 1268–1278.

Moonan, F., Molina, J., Mirkov, T.E., 2000. Sugarcane yellow leaf virus: an emerging virus that has evolved by recombination between luteoviral and poleroviral ancestors. Virology 269, 156–171.

Morel, J.B., Godon, C., Mourrain, P., Beclin, C., Boutet, S., Feuerbach, F., Proux, F., Vaucheret, H., 2002. Fertile hypomorphic ARGONAUTE (ago1) mutants impaired in post-transcriptional gene silencing and virus resistance. Plant Cell 14, 629–639.

Mourrain, P., Beclin, C., Elmayan, T., 2000. *Arabidopsis* SGS2 and SGS3 genes are required for posttranscriptional gene silencing and natural virus resistance. Cell 101, 533–542.

Palauqui, J.C., Vaucheret, H., 1998. Transgenes are dispensable for the RNA degradation step of cosuppression. Proc. Natl. Acad. Sci. U. S. A. 95, 9675–9680.

Pazhouhandeh, M., Dieterle, M., Marrocco, K., Lechner, E., Berry, B., Brault, V., Hemmer, O., Kretsch, T., Richards, K.E., Genschik, P., Ziegler-Graff, V., 2006. F-box-like domain in the polerovirus protein P0 is required for silencing suppressor function. Proc. Natl. Acad. Sci. U. S. A. 103, 1994–1999.

Pfeffer, S., Dunoyer, P., Heim, F., Richards, K.E., Jonard, G., Ziegler-Graff, V., 2002. P0 of beet Western yellow virus is a suppressor of posttranscriptional gene silencing. J. Virol. 76, 6815–6824.

Rott, P., Mirkov, T.E., Schenck, S., Girard, J.C., 2008. Recent advances in research on *Sugarcane yellow leaf virus*, the causal agent of sugarcane yellow leaf. Sugar cane Int. 26, 18–27.

Schenk, S., Hu, J.S., Lockhart, B.E., 1997. Use of a tissue blot immunoassay to determine the distribution of sugarcane yellow leaf virus in Hawaii. Sugar Cane 4, 5–8.

Siemering, K.R., Golbik, R., Sever, R., Haseloff, J., 1996. Mutations that suppress the thermosensitivity of green fluorescent protein. Curr. Biol. 6, 1653–1663.

Smith, G.R., Borg, Z., Lockhart, B.E.L., Braithwaite, K.S., Gibbs, M.J., 2000. Sugarcane yellow leaf virus: a novel member of the *Luteoviridae* that probably arose by inter-species recombination. J. Gen. Virol. 81, 1865–1869.

Takeda, A., Sugiyama, K., Nagano, H., Mori, M., Kaido, M., Mise, K., Tsuda, S., Okuno, T., 2002. Identification of a novel RNA silencing suppressor, NSs protein of Tomato spotted wilt virus. FEBS Lett. 532, 75–79.

van der Wilk, F., Houterman, P., Molthoff, J., Hans, F., Dekker, B., van den Heuvel, J., Huttinga, H., Goldbach, R., 1997. Expression of the potato leafroll virus ORF0 induces viral-disease-like symptoms in transgenic potato plants. Mol. Plant-Microbe Interact 10, 153–159.

Vaucheret, H., Beclin, C., Elmayan, T., Feuerbach, F., Godon, C., Morel, J.B., Mourrain, P., Palauqui, J.C., Vernhettes, S., 1998. Transgene-induced gene silencing in plants. Plant J. 16, 651–659.

Vega, J., Scagliusi, S.M.M., Eugênio, C.U., 1997. Sugarcane yellow leaf disease in Brazil: evidence of association with a luteovirus. Plant Dis. 81, 21–26.

Voinnet, O., 2005. Non-cell autonomous RNA silencing. FEBS Lett. 579, 5858–5871.

Voinnet, O., Vain, P., Angell, S., Baulcombe, D., 1998. Systemic spread of sequence-specific transgene RNA degradation in plants is initiated by localized introduction of ectopic promoterless DNA. Cell 95, 177–187.

Wassenegger, M., Krczal, G., 2006. Nomenclature and functions of RNA-directed RNA polymerases. Trends Plant Sci. 11, 42–151.

Xie, Z., Allen, E., Wilken, A., Carrington, J.C., 2005. DICER-LIKE 4 functions in trans-acting small interfering RNA biogenesis and vegetative phase change in *Arabidopsis thaliana*. Proc. Natl. Acad. Sci. U. S. A. 102, 12984–12989.

Yang, L., Huang, W., Wang, H., Cai, R., Xu, Y., Huang, H., 2006. Characterization of a hypomorphic *argonaute1* mutant reveal novel *AGO1* functions in *Arabidopsis* lateral organ development. Plant Mol. Biol. 61, 63–78.

Zhang, X., Du, P., Lu, L., Xiao, Q., Wang, W., Cao, X., Ren, B., Wei, C., Li, Y., 2008. Contrasting effects of HC-Pro and 2b viral suppressors from Sugarcane mosaic virus and Tomato aspermy cucumovirus on the accumulation of siRNAs. Virology 374, 351–360.